THE USE OF CONDUCTIVE NANOMATERIAL-DECORATED FILTERS FOR IMPROVEMENT OF INDOOR AIR QUALITY BY PARTICULATE MATTER FILTRATION

A THESIS SUBMITTED TO
THE GRADUATE SCHOOL OF NATURAL AND APPLIED SCIENCES
OF
MIDDLE EAST TECHNICAL UNIVERSITY

BY

MELEK HAZAL BAŞKÖY

IN PARTIAL FULFILLMENT OF THE REQUIREMENTS
FOR
THE DEGREE OF MASTER OF SCIENCE
IN
ENVIRONMENTAL ENGINEERING

AUGUST 2022

Approval of the thesis:

THE USE OF CONDUCTIVE NANOMATERIAL-DECORATED FILTERS FOR IMPROVEMENT OF INDOOR AIR QUALITY BY PARTICULATE MATTER FILTRATION

submitted by **MELEK HAZAL BAŞKÖY** in partial fulfillment of the requirements for the degree of **Master of Science** i**n Environmental Engineering, Middle East Technical University** by,

Prof. Dr. Halil Kalıpçılar
Dean, Graduate School of **Natural and Applied Sciences** _____

Prof. Dr. Bülent İçgen
Head of the Department, **Environmental Eng.** _____

Prof. Dr. Tuba Hande Bayramoğlu
Supervisor, **Environmental Eng., METU** _____

Prof. Dr. Hüsnü Emrah Ünalan
Co-Supervisor, **Met. and Mat. Eng. , METU** _____

Examining Committee Members:

Prof. Dr. Ayşegül Aksoy
Environmental Engineering, METU _____

Prof. Dr. Tuba Hande Bayramoğlu
Environmental Engineering, METU _____

Prof. Dr. Hüsnü Emrah Ünalan
Metallurgical and Materials Engineering, METU _____

Prof. Dr. Gülen Güllü
Environmental Engineering, Hacettepe University _____

Assist. Prof. Dr. Simge Çınar Aygün
Metallurgical and Materials Engineering, METU _____

Date: 19.08.2022

I hereby declare that all information in this document has been obtained and presented in accordance with academic rules and ethical conduct. I also declare that, as required by these rules and conduct, I have fully cited and referenced all material and results that are not original to this work.

Name Last name : Melek Hazal Başköy

Signature :

ABSTRACT

THE USE OF CONDUCTIVE NANOMATERIAL-DECORATED FILTERS FOR IMPROVEMENT OF INDOOR AIR QUALITY BY PARTICULATE MATTER FILTRATION

Başköy, Melek Hazal
Master of Science, Environmental Engineering
Supervisor: Prof. Dr. Tuba Hande Bayramoğlu
Co-Supervisor: Prof. Dr. Hüsnü Emrah Ünalan

August 2022, 99 pages

Particulate matter (PM) is one of the six criteria air pollutants that is of greatest concern to air quality. In order to control PM pollution, highly effective air filters are required. The shortcomings of conventional filtration methods have led to the development of effective filtration strategies. In this study, the utilization of two different nanomaterial-decorated nylon mesh filters was investigated. Silver nanowire (Ag NW) and two-dimensional titanium carbide ($Ti_3C_2T_x$) MXene were selected due to their high electrical conductivity as well as their high specific surface area. The performances of the filters at different air velocities (0.45 m/s and 1.02 m/s) and voltages (2.5 V, 5 V, 7.5 V, and 10 V) were investigated. The best PM removal performance for both filter types was obtained when the applied voltage was 10 V and the air velocity was 1.02 m/s. Ag NW-decorated filters had mass concentration-based removal efficiencies of 90.98% and 96.11% for $PM_{2.5}$ and PM_{10}, respectively. They showed number concentration-based removal efficiencies of 70.98% and 71.21% for $PM_{2.5}$ and PM_{10}, respectively. Based on mass concentration, MXene-decorated filters had removal efficiencies of 90.05% and 95.44% for $PM_{2.5}$

and PM_{10}, respectively. They showed number concentration-based removal efficiencies of 70.37% and 70.58% for $PM_{2.5}$ and PM_{10}, respectively. Since air filters with multifunctional performance are desired, tests of some parameters (reusability, repeatability, and 2-hour filtration) were also carried out. Considering the observed removal efficiencies, low pressure drops, and multifunctional performances, these nanomaterial-decorated filters are promising filters for air filtration, but improvements are still needed.

Keywords: Air pollution, Particulate matter, Air filtration, Silver nanowires, MXene

ÖZ

PARTİKÜL MADDE FİLTRASYONU İLE İÇ HAVA KALİTESİNİN İYİLEŞTİRİLMESİ İÇİN İLETKEN NANOMATERYAL DEKORE EDİLMİŞ FİLTRELERİN KULLANILMASI

Başköy, Melek Hazal
Yüksek Lisans, Çevre Mühendisliği
Tez Yöneticisi: Prof. Dr. Tuba Hande Bayramoğlu
Ortak Tez Yöneticisi: Prof. Dr. Hüsnü Emrah Ünalan

Ağustos 2022, 99 sayfa

Partikül madde (PM), hava kalitesiyle ilgili en büyük endişe kaynağı olan altı kriter hava kirleticisinden biridir. PM kirliliğini kontrol etmek için son derece etkili hava filtreleri gereklidir. Geleneksel filtrasyon yöntemlerinin eksiklikleri, etkili filtreleme stratejilerinin geliştirilmesine yol açmıştır. Bu çalışmada, iki farklı nanomalzeme kaplı naylon ağ filtrenin kullanımı araştırılmıştır. Gümüş nanotel (Ag NW) ve iki boyutlu titanyum karbür ($Ti_3C_2T_x$) MXene, yüksek elektriksel iletkenlikleri ve yüksek özgül yüzey alanları yüzünden seçilmiştir. Farklı hava hızlarına (0.45 m/s ve 1.02 m/s) ve farklı voltajlara (2.5 V, 5 V, 7.5 V, 10 V) sahip filtrelerin değişen performansları araştırılmıştır. Her iki filtre için de en iyi PM giderme performansı, uygulanan voltaj 10 V ve hava hızı 1.02 m/s iken elde edilmiştir. Ag NW kaplı filtreler, $PM_{2.5}$ ve PM_{10} için sırasıyla %90.98 ve %96.11 kütle konsantrasyonuna dayalı giderim verimliliğine sahiptir. Bu filtreler, $PM_{2.5}$ ve PM_{10} için sırasıyla sayı konsantrasyonuna dayalı %70.98 ve %71.21 giderim verimliliğine sahiptir. MXene kaplı filtreler, $PM_{2.5}$ ve PM_{10} için sırasıyla %90.05 ve %95.44 kütle konsantrasyonuna dayalı giderim verimliliğine sahiptir. Bu filtreler, $PM_{2.5}$ ve PM_{10}

için sırasıyla sayı konsantrasyonuna dayalı %70.37 ve %70.58 giderim verimliliğine sahiptir. Çok fonksiyonlu performansa sahip hava filtreleri istendiği için bazı parametrelerin (yeniden kullanılabilirlik, tekrarlanabilirlik, ve 2-saat filtrasyon) testleri de yapılmıştır. Gözlenen giderim verimleri, düşük basınç düşüşleri ve çok işlevli performanslar göz önüne alındığında, bu nanomalzemeler ile dekore edilmiş filtreler, hava filtrasyonu için umut verici filtrelerdir, ancak hala iyileştirmelere ihtiyaç vardır.

Anahtar Kelimeler: Hava kirliliği, Partikül madde, Hava filtrasyonu, Gümüş nanoteller, MXene

ACKNOWLEDGEMENTS

First and foremost, I would like to thank and express my deepest gratitude to my advisor Prof. Dr. Tuba Hande Bayramoğlu for her valuable guidance, patience, professional advice, and encouragement throughout my studies. I would also express my appreciation to my co-advisor Prof. Dr. H. Emrah Ünalan for his valuable recommendations and support.

I owe my appreciation to Prof. Dr. Gürdal Tuncel for his valuable contributions and support.

I would like to acknowledge all people in Envbiorg group and METE Nanolab group for their help throughout this thesis.

I also would like to thank AFT Filtre for supplying me a HEPA filter.

Most importantly, I would like to express my biggest appreciation to my wonderful parents Necla Başköy and Selami İlker Başköy, and my lovely brother Efe Başköy for their unconditional and endless love, support throughout my life. I am always proud to be a part of this family.

Finally, I owe my special thanks to my love, Burak Özen. Thank you for all your endless support, trust, patience, and love. I feel very excited to share the same surname soon. Thank you for always being there.

TABLE OF CONTENTS

LIST OF TABLES

TABLES

LIST OF FIGURES

FIGURES

LIST OF ABBREVIATIONS

ABBREVIATIONS

Ag NP	Silver Nanoparticle
Ag NW	Silver Nanowire
BC	Black Carbon
COPD	Chronic Obstructive Pulmonary Disease
CCN	Cloud Condensation Nuclei
EDM	Environmental Dust Monitor
EDS	Energy Dispersive Spectroscopy
EG	Ethylene Glycol
EHD	Electro-hydrodynamic Jet
FT- IR	Fourier Transform Infrared Spectrophotometry
HEPA	High Efficiency Particulate Air
IPPC	Intergovernmental Panel on Climate Change
LAS	Laser Aerosol Spectrometry
MDNM	MXene Decorated Nylon Mesh
MPPS	Most Penetrating Particle Size
OLED	Organic Light Emitting Diodes
PAN	Polyacryonitrile
PM	Particulate Matter
PM_1	Particulate matter with an aerodynamic diameter of up to 1 μm
$PM_{2.5}$	Particulate matter with an aerodynamic diameter of up to 2.5 μm
PM_{10}	Particulate matter with an aerodynamic diameter of up to 10 μm
PVP	Polyvnylpyrolidone
SSA	Sea Spray Aerosols
SEM	Scanning Electron Microscopy
ULPA	Ultra Low Particulate Air
USEPA	United States Environmental Protection Agency
WHO	World Health Organization

CHAPTER 1

INTRODUCTION

The rapid development of urbanization and industrialization with the increasing population in the world, the proliferation of pesticides and harmful chemicals, and the increase in the use of motor vehicles have caused serious environmental problems. One of these problems is air pollution, which is increasing day by day and is a global threat. According to the World Health Organization (WHO), about 8 million people die prematurely every year due to diseases (pneumonia, chronic obstructive pulmonary disease, lung cancer, etc.) that may be related to air pollution (WHO, 2016). 4.2 million of these deaths are caused by effects of outdoor air pollution, both in cities and in rural areas, and 3.8 million by indoor air pollution (WHO, 2016).

Air quality is determined by the concentrations of pollutants including particulate matter (PM), nitrogen oxides (NO_x), sulfur oxides (SO_x), carbon monoxide (CO) and carbon dioxide (CO_2). As one of these pollutants, PM is a mixture of solid and liquid particles including carbon, heavy metals, polycyclic aromatic hydrocarbon derivatives, soil particles, sea salt, and radioactive substances suspended in the air. PM is one of the six criteria air pollutants with defined concentration limits that distinguish acceptable air quality from poor or unhealthy air quality. The chemical and physical properties of PM are related to the size of the particles, the region where it is located, and the emission source (Yadav and Devi, 2019). Accordingly, United States Environmental Protection Agency (USEPA) classified PM as particles smaller than 0.1 μm in diameter (PM_1), particles smaller than 2.5 μm in diameter ($PM_{2.5}$), and particles smaller than 10 μm in diameter (PM_{10}) (USEPA, 2007a). Especially in smaller sizes, PM can easily penetrate the bronchi and lungs; even short-term exposure can cause chronic respiratory diseases such as lung cancer, asthma, chronic

obstructive pulmonary disease (COPD), bronchitis, and cardiovascular diseases (Vijayan et al., 2015).

Due to the COVID-19 pandemic, which has been on the world agenda for the last 2 years, the importance of indoor air quality has increased as most people spend about 80-90% of their time indoors (school, home, gym, office, etc.). As pollutant transfer occurs between indoor and outdoor environments during air exchange (Lv and Zhu, 2013), PM becomes a carrier of chemicals used inside or adsorbed on particles outside (Narcı, 2017). However, since PM can act as a carrier to which viruses can cling, it is thought that high levels of PM in the atmosphere may increase the rate of spread of viruses (Harrod et al., 2003). To control indoor air pollution, pollutants can be minimized at the source, ventilation systems can be improved, or the use of air purifiers can be expanded. Air purifiers generally use a multi-layer filter system consisting of a pre-filter, a carbon filter, an antibacterial filter, and a high efficiency air particulate (HEPA) filter (Vijayan et al., 2015).

Efficient air filtration, one of the methods applied to improve indoor air quality, can reduce the symptoms of diseases that can be caused by PM. Porous filters and fibrous filters are two common types of air filtration materials. Porous filters are made by creating pores in solid substrates to capture PM. However, as the collected particles will clog the pores at the filter inlet over time, the filtration performance will decrease and therefore the pressure drop between the inlet and outlet of the filters will increase (Zhao et al., 2017). The other filtration type, fibrous filters, capture PM through physical barriers and surface adhesion (Xiao et al., 2018). High surface area is highly desirable in fibrous filters, as more PM would be captured if the surface area were larger (Jung et al., 2018). However, it is more difficult to maintain high-efficiency filtration cost effectively for long service life in fibrous filters (Liu et al., 2020). The drawbacks of traditional filtration techniques have led to an increase in the efforts to develop an effective strategy for PM removal. When evaluating the filter material, which is the most important factor affecting the filtration performance, various

parameters such as removal efficiency, pressure drop, thermal stability, specific surface area, and optical transmittance are used (Liu et al., 2020). Filters should be easily accessible, inexpensive, and easily reusable. In addition, antibacteriality is a desired property in air filters, as bacteria can be a portion of respirable microorganisms in PM (Wang et al., 2016). Thus, diseases caused by air conditioning and ventilation systems (such as Legionnaires' disease) can be minimized.

With the development of nanotechnology, the use of one-dimensional (i.e. nanowires), two-dimensional (i.e. graphene and graphene oxide), and three-dimensional (i.e. nanoparticles, nanofiber) nanomaterials in different fields of environmental engineering has begun to attract more attention. Silver nanowire (Ag NW) is defined as a one-dimensional nanomaterial made up of pure silver with diameters and lengths typically in the range of 10-200 nm and 5-100 μm, respectively (Bahçelioğlu et al., 2019). The most extensively investigated two-dimensional materials for the removal of various environmental contaminants are graphene and graphene oxide derivatives. Recently, transition metal carbides and nitrides, called MXenes, have emerged as candidate two-dimensional materials. Ag NW and titanium-based MXenes hold promise for various environmental applications such as water treatment (Bahçelioğlu et al., 2019; Ding et al., 2018; Pandey et al., 2018). These nanomaterials could be useful for air purification because of several desirable properties, including high surface area. The number of studies conducted using silver nanoparticles (Ag NP) and Ag NWs have increased in the last decade and have shown positive results in PM removal (Jeong et al., 2017; Huang et al., 2019). However, there are limited studies focused on this subject. Compared to commercial air filters, conductive nanomaterial-decorated filters may be promising. The developed filters can reach high efficiencies with lower pressure drops. Thus, they can be used in air purifiers or in air conditioners where HEPA filters are frequently used. Moreover, unlike the one used in these products, developed nanomaterial-decorated filters can effectively remove particles with a single-layer structure.

1.1 Scope of Thesis

This thesis aims to improve the indoor air quality. Therefore, the scope of this thesis was to develop an alternative product to the filter industry with high filtration performance including high PM removal efficiency, low pressure drop, and energy efficiency. With this scope, two different filters were produced. In the first one Ag NWs were decorated onto nylon filters, whereas in the second one MXenes were decorated. Nylon mesh was selected as the filter material for reasons such as large openings, easy accessibility, cheapness, and lightness. It can be coated with nanomaterials even though it has large openings (Jeong et al., 2017; Han et al., 2021a). While traditional systems use a multi-layer filtration system, developed filters might show its efficiency even in single-layer use.

The specific objectives of this thesis are given as follows:

- To investigate the effect of voltage application on nanomaterial-decorated filters in PM filtration performance,
- To investigate the filtration performance of both filter types at different air velocities,
- To investigate the filtration performances of both filter types for parameters namely, reusability, repeatability, and 2-hour filtration performance.

CHAPTER 2

LITERATURE REVIEW

2.1 Air pollution

Air, which consists of mixtures of gases that make up the atmosphere, is one of the most important elements for living things. Air pollution, which is a global environmental problem, is defined by the USEPA as pollution caused by chemical, physical or biological factors in the indoor and outdoor environment by disrupting the natural properties of the atmosphere (USEPA, 2007b). Although the atmosphere has the ability to neutralize the harmful substances in it with its natural mechanisms, it is constantly polluted due to the increasing emissions.

Air pollutants are emitted from various sources and spread into the atmosphere via different mechanisms. While some of them are destroyed naturally, the part that deposits to the Earth surface poses a danger to the ecosystem and living organisms.

Air pollution is classified as either indoor (household) air pollution or outdoor (ambient) air pollution. Although there are gases and particles released as a result of natural processes such as volcanic activities, sandstorms etc., it has been determined that emissions resulting from the combustion of fossil fuels used in domestic heating, industrial facilities, motor vehicles and energy production are the main cause of air pollution. Residences, schools, offices, shopping malls, hospitals, restaurants, etc., where people spend most of their time, are considered indoor environments. The pollution caused by the pollutants in these environments is called indoor air pollution. In addition to the leakage of particles that create outdoor air pollution into the indoor environment, pollutants released from cooking and heating activities, smoking, painting, using deodorants and room fragrances, and construction and

insulation materials also contribute to indoor air pollution. USEPA has stated that indoor air pollutant levels are usually 2 to 5 times higher than outdoor pollutant levels (Wallace et al., 1986). This can be attributed to the fact that indoor areas allow pollutants to accumulate more than outdoor areas (Kankaria et al., 2014) and the exposure time to indoor air pollution is longer.

The standards that show acceptable concentration values of the pollution in the atmosphere are called air quality standards. In order to protect the environment and human health, criteria air pollutants, namely, particulate matter (PM), ground-level ozone (O_3), carbon monoxide (CO), sulfur dioxide (SO_2), nitrogen dioxide (NO_2), and lead (Pb), have determined (Saxena and Sonwani, 2019).

2.2 Particulate matter (PM)

Particulate matter (PM), one of the six criteria pollutant defined by the USEPA, is the name given to a complex mixture of solid or liquid particles that can remain suspended in the air for some time. Atmospheric PM, which is one of the pollutants with the greatest negative effects on human health, consists of various inorganic and organic substances. These substances may be elemental carbon, ammonium, nitrates, sulfates, minerals, and trace elements (World Health Organization, 2021).

The properties of the atmospheric particles vary depending on their formation and source, their size, and the components they contain. Since atmospheric particles have sizes ranging from tens of micrometers to nanometers, it is important to define the size of PM in order to make evaluations about their physical and chemical properties, transformation, transport and removal from the atmosphere.

The aerodynamic diameter is used to calculate PM size because not all particles in the air are spherical and uniformly shaped. The diameter of a spherical particle with a unit density and the same inertial characteristics (i.e. settling velocity) with the

particle of interest is expressed as the aerodynamic diameter (Aramendia et al., 2018). The average aerodynamic diameter of airborne particles ranges from about 0.002 μm to 100 μm and is divided into three classes according to their size: PM_1 (particles, smaller than 0.1 μm in aerodynamic diameter), $PM_{2.5}$ (particles smaller than 2.5 μm in aerodynamic diameter), and PM_{10} (particles smaller than 10 μm in aerodynamic diameter). Within the scope of meeting air quality standards, $PM_{2.5}$ and PM_{10} are regularly measured and monitored.

2.2.1 Sources of PM

PM sources can both be primary (directly released to the atmosphere) or secondary (indirectly released to the atmosphere via conversion into condensable species as particles as a result of chemical reactions) (National Research Council, 2010). In a recent study in Eastern Mediterranean, it was demonstrated that almost all PM_1 particles are secondary particles in rural atmosphere, but have a significant primary component in urban atmosphere (Uzunpınar, 2022).

Airborne PM can be made up of hundreds of different chemicals from either natural and anthropogenic sources. These particles spread into the atmosphere in very different sizes and ways. The deposition and the size of the PM are affected by the source. Although natural sources cause more of the atmospheric PM by weight, PM emitted from anthropogenic sources is more dangerous for both human and ecosystem health (Carruthers et al., 2005; National Research Council, 2010). Also, anthropogenic sources generally cause the release of small particles. This is because the abundance and atmospheric lifetime of an airborne particle is inversely proportional to its aerodynamic diameter.

Among natural sources, mineral dust, volcanic activities, wildfires, sea spray aerosols (SSA), biological agents (bacteria, viruses, fungi, algae, etc.), and particles released into the atmosphere by vegetation are located. Mineral dust dispersed by the

wind and soil erosion can be attributed to the largest portion of naturally originated PM_{10} emissions. Dust emitted from desert areas around the world, particularly from Sahara, is the biggest contributor for these emissions (Fuzzi et al., 2015). Volcanic eruptions and ash from volcanic activities are considered another source of naturally occuring PM. Wildfires, which are not caused by humans and occur as a result of spontaneous combustion of organic materials in nature, increase the carbon mass and cause an increase in the amount of PM. Sea spray aerosols, formed by bubble bursting process at the ocean surface, are also a component of PM emissions. There is a wide range of small biological pollutants such as viruses, protozoa, bacteria etc., which humans are inevitably exposed, are usually found in humid environments and may be responsible for a portion of air pollution. Secondary organic particles consisting of long-chain hydrocarbons formed from volatile organic compounds emitted from vegetation, particularly from trees in forest, which are known as "terpenes" also makes up a significant component in naturally emitted particles.

Anthropogenic sources include residential heating, industrial activities and mobile sources (i.e. cars, motorcycles, aircrafts, ships, and railway vehicles etc.). Fossil fuel consumption by various purposes is the biggest contributor to the air pollution. PM emission from domestic heating occurs as a result of the combustion or incomplete combustion of low-quality fuels with low calories, high sulfur, volatile organic compounds, and ash content (i.e. coal and wood). Major industries related to PM emissions include thermal power plants, cement production, quarries, metal industries such as iron and steel foundry, construction activities, mining, and agricultural activities. As a result of these activities, heavy metals and trace elements are emitted to the atmosphere. On the other hand, mobile sources create an important part of particle emissions. As the number of vehicles traveling in traffic increases and the vehicle speed decreases, the amount of pollutants released from the exhaust also increases. Vehicles that do not have periodic vehicle maintenance and inspection for emission measurement, public transportation vehicles carrying loads above their capacity, vehicles that are over 20 years old, and vehicles that use unsuitable fuels in

the vehicle engine increase the emission of PM pollutants. Especially motor vehicles using diesel fuel generate more PM_{10} than gasoline vehicles (Dorjsuren, 2012). Diesel vehicles attracted special attention in recent years, because they are an important source of black carbon, which is a significant contributor to global warming, in atmosphere.

A wide variety of other sources of PM should be considered, which can also be originated through windows and doors opening to the outside environment, resulting in various compositions of particle mass and particle size distributions in indoor environment. Combustion processes, in particular, are among the important sources of PM for both indoor and outdoor environments. Indoor pollutants often come from cleaning activities, repair and painting operations, cooking, smoking, use of deodorizing sprays or air fresheners, and keeping furry pets. It is also possible that PM can spread from household materials such as furniture, wood, carpets, adhesives, houseplants and bathroom materials (Karakaş, 2015).

2.2.2 Health and environmental effects of PM

There are various effects of PM-based air pollution on health and environment. Air pollution, which causes serious problems for all living things, has been shown as the 13th cause of death worldwide according to the World Health Organization, and it has been stated that approximately 800,000 people die every year due to air pollution caused by PM (Polichetti et al., 2009). According to the results of studies during recent decades on the effects of PM on human health, the levels of $PM_{2.5}$ and PM_{10} are regulated. Provided in Table 2.1, there is no limit value for $PM_{2.5}$ standard in Turkey.

Table 2.1 Average standard and recommendation values for PM.

Pollutant	Period	WHO's recommended value[a]	Turkey's regulation value[b]
PM_{10}	24 hour	50 $\mu g/m^3$	50 $\mu g/m^3$
	Annual	20 $\mu g/m^3$	40 $\mu g/m^3$
$PM_{2.5}$	24 hour	25 $\mu g/m^3$	-
	Annual	10 $\mu g/m^3$	-

[a]WHO global air quality guidelines: particulate matter ($PM_{2.5}$ and PM_{10}), ozone, nitrogen dioxide, sulfur dioxide and carbon monoxide (https://www.who.int/publications/i/item/9789240034228).

[b]Hava Kalitesi Değerlendirme ve Yönetimi Yönetmeliği (https://www.mevzuat.gov.tr/mevzuat?MevzuatNo=12188&MevzuatTur=7&MevzuatTertip=5).

PM enters the human body in three different ways, these are respiratory, skin, and food routes. Since the most basic of these exposure routes is the respiratory tract, the most important health effects of PM are also seen in the respiratory system. The accumulation places of the particles in the respiratory organs and their residence time depend on the organic/inorganic components and concentrations, and the size of PM, and the health and age status of the exposed person. Pregnant women, elderly people, people with heart and lung diseases, and children constitute risky groups. Numerous studies demonstrate that children are more vulnerable than adults to health problems caused by PM, since their breath rates are higher than adults and their respiratory systems are not fully evolved (D'Amato et al., 2015). Long-term exposure to air pollutants at low concentrations and short-term exposure to high concentrations can cause serious health problems. Acute effects such as sore throat and cough can be seen as a result of short-term exposure to PM. Meanwhile, diseases such as bronchitis, COPD, and aggravated asthma can be attributed to the long-term exposure of PM. In addition, PM can contain heavy metals such as mercury, lead, cadmium and carcinogenic chemicals, and increase the harmful effects of these substances by delivering other pollutants adsorbed on their surfaces to sensitive

living tissues at higher than normal concentrations in the air (Kahramantekin, 2006). These chemicals combine with moisture to turn into acids, so when these pollutants are together, the negative effects on health are greater than the effects of each individually. Therefore, it is of great importance to know the size, number and chemical composition of the particles in order to detect the health effects of PM.

The most important criterion in evaluating the potential effects of PM on health is the aerodynamic diameter of the particles, which varies from nanometer to micrometer.

Table 2.2 shows the relationship between particle size and effect of particles on respiratory system. In a study conducted on this subject, 10 $\mu g/m^3$ daily increase in PM_{10} concentration have increased the death rate by 0.51% (Samet et al., 2000). In another study, it was stated that 10 $\mu g/m^3$ increase in $PM_{2.5}$ exposure increased the risk of death by 8-18% (Taner et al., 2011).

Although PM_{10} appears to be less harmful due to its relatively short atmospheric lifetime and mostly uptake by the nose and upper respiratory tract, it has significant effects on human health, especially at high concentrations. Epidemiological studies have found links between the increase in PM concentrations and cardiovascular system diseases and mortality. However, PM_{10} has also been associated with heart arrhythmias and heart attacks, as it reaches the lungs and slows the conversion of carbon dioxide in the blood to oxygen, causing shortness of breath (Koçak, 2006; Polichetti et al., 2009; Scherbakova, 2010).

Small-sized particles such as $PM_{2.5}$ and PM_1 are more dangerous in their effects than coarse particles. Particles ranging in size from 0.01 μm to 4 μm, especially from cigarette smoke and motor vehicle exhausts, can penetrate deeper into the lungs and even reach the bloodstream, causing a longer accumulation time in the alveoli (Müezzinoğlu, 2005). The accumulation of fine particles in the alveoli constitutes a

very risky situation, since there are no hairs to capture the particles in this region. Particularly, particles with a diameter of less than 0.1 μm reach the capillary air pipes in the lungs owing to the Brownian movement, settle in the air sacs called alveoli and stay in this area for a long time (Taner, 2012). Researches indicated that $PM_{2.5}$ can cause increases in pulmonary heart diseases, respiratory diseases such as asthma, COPD etc., cardiovascular diseases, inflammatory diseases, allergic diseases, cancer, premature births, hypertension, skin aging, and even the mortality (Lin et al., 2018). In addition, $PM_{2.5}$ exposure might also negatively affect the mental health and increase the risk of mental disorder (Xue et al., 2020).

Table 2.2 The effect of different sized-particles on respiratory system (Scherbakova, 2010).

Particle size	**Effect on respiratory system**
>11 μm	Does not enter
7-11 μm	Trapped in nose
4.7-7 μm	Trapped in throat
3.3-4.7 μm	Trapped in trachea and primary bronchi
2.1-3.3 μm	Trapped in secondary bronchi
1.1-2.1 μm	Trapped in tertiary bronchi
0.65-1.1 μm	Trapped in bronchial tube
0.43-0.65 μm	Trapped in pulmonary alveolus

PM has effects on environment beside human health, since it can be carried over long distances before settling on a surface which might be ground or water. These impacts include visibility reduction, impacts on climate by cloud condensation nuclei (CCN) formation, changes in the vegetation and ecosystems caused by the alteration of the

nutrient balance, climate change contributed by the black carbon (BC), and aesthetical damage.

Visibility is denoted as the maximum distance that can be seen with the unaided eyesight. Since the scattering and absorption of visible light by suspended particles is the main cause of visibility impairment (haze), small particles such as PM_1, $PM_{2.5}$ can be blamed for the problem. Transport safety is compromised as a result of reduced visibility caused by high PM concentrations attributable to anthropogenic sources such as power plant emissions, fuel emissions, and industries.

Particles that will act as nuclei at a certain supersaturation are essential in the formation of water droplets necessary for the formation of the hydrological cycle. CCN, are small particles in the air that are main stones to initiate vapor condensation in the formation of cloud, rain as well as other precipitation forms. Examples of CCNs, also known as cloud seeds, are mineral dusts, soot from fires, volcanic ash, SSA, sulfates released by phytoplankton in the aquatic ecosystems, vehicle exhaust, pollen and organic aerosols released by plants. However, large amounts of CCN result in the formation of haze or smog, the destruction of stratospheric ozone, and the alteration of abundance and distribution of atmospheric trace gases by chemical reactions.

As the air particles settle on the surfaces after a while, PM with various chemical composition affects ecological systems in many ways. When PM pollution exists in a natural area such as forest, wildlife, or coastal regions, it affects the metabolic processes (i.e. photosynthesis) of plants, soil metal concentration and thus salinity, animal growth, acidification of lakes and streams, and diversity of ecosystems. When a river becomes acidic as a result of contamination with PM, it endangers the lives of sensitive creatures living in the aquatic environment, and inhibits the growth of trees since vital nutrients for trees to remain leached out in the soil. All these formations lead to a decrease in biodiversity.

Air pollution and climate change are intimately connected to each other by various interactions. With its effect on earth's radiative budget, PM might be the airborne pollutant that best describes air quality and climate change interaction. From 1860 to 2000, the global population-based $PM_{2.5}$ concentrations increased by 5% due to climate change (Fang et al., 2013). Aerosols that reflect sunlight are usually particles with a low carbon content and cool the earth's surface. Aerosols absorbing sunlight are particles that are generally formed as a result of combustion processes. Black Carbon (BC), is the strong light-absorbing fraction of fine particles. Because of this ability, Intergovernmental Panel on Climate Change (IPCC) considered BC as the second major contributor to climate change. BC affects climate by different ways such as albedo effect. BC is accumulated on the snow and ice, absorbing more sunlight, causing more glaciers to melt. Besides, it may generate heat in atmosphere, causing change on precipitation patterns. When it is deposited on plant leaves, it may disrupt the forests by increasing their temperature.

In terms of aesthetic damage, all airborne particles can be considered a threat, especially for objects of historical value such as monuments. PM causes the object to become soiled or corroded and therefore aesthetically damaged. Chemical reactions, especially between large amounts of PM and other harmful compounds, can cause further damage by changing the structure of materials. Also, the probability of damage increases when the particles are wet or in the liquid phase (Gysels et al., 2002).

2.2.3 PM filtration

Interactions between particle and filter material has a significant impact on the filtration process. Since the sizes of the particles in the atmosphere vary, many filtration methods are needed. When simple filtration theories are used to explain complex filtration processes, analyzing the collection of the particle over a single fiber emerges as an easy method (Büyüknalçacı, 2018). Basically, mechanisms such

as gravity, inertia, interception, diffusion and electrostatic attraction have contributed to the capturing of particles (Liu et al., 2020). The relevant particle ranges and schematics of the filtration methods explained according to the preferred flow direction of the fiber are displayed in Figure 2.1. In order to produce an efficient filter, multiple filtration mechanism should be utilized by taking into consideration of particle size and density, fiber thickness, and air velocity.

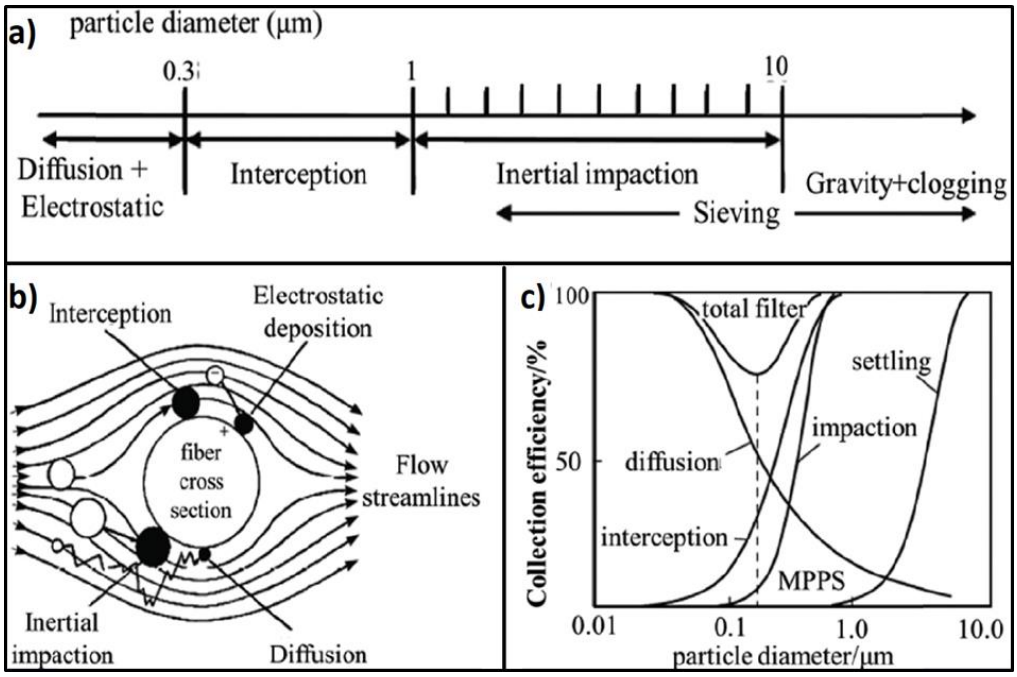

Figure 2.1 (a) Filtration effect based on particle size, (b) Filtration mechanisms, (c) Filtration efficiency based on particle size (Barhate et al., 2007; Ding et al., 2018).

Straining or sieving method, which can be defined as the simplest mechanism and used for coarse particles, is the separation of particles whose diameter is larger than the pore size of the filtration material (Dökmen, 2011).

In inertial impaction method, which is another method used to filter large particles, the particles are separated from the air stream by the gravitational force. The particles continue on their way by turning around the filtration material without breaking their parallelism. However, the particles entrained in the flow cannot rotate around the

filter material due to their inertia and weight, hitting the fiber and can be filtered from the airstream. This effect is directly proportional to the air velocity and particle diameter and inversely proportional to the pore diameter of the filter material.

Interception, also known as contact or hook, involves capturing particles with smaller sizes. These particles are light enough to follow the streamline but if the streamline passes closer to the fiber than the particle diameter in the movement of the particle around the fiber, the particle is caught by the fiber and is removed from the air. Interception is generally more efficient when particle size decreases. Interception differs from inertial impaction in that there is no divergence from the center streamline for an interception, where the filter material intercepts the particle (Mahdavi, 2013).

The Brownian diffusion principle, which is the most complex mechanism in air filtration mechanism to explain, is efficient for very light particles smaller than 0.3 μm in diameter, which move irregularly, do not follow a smooth route, such as gas molecules. Since most of the airborne particles are submicron, this principle is of great importance in air filtration technique and is mostly used in medium and high efficiency expanded surface filters. In order to provide an effective filtration, a large number of particles must be able to collide with the media fibers thanks to the molecular attraction force called the Van der Waals force. In this case, the principle will become more efficient as the air velocity, particle diameter and fiber diameter decrease.

Conventional air filters can passively provide a high PM removal efficiency with the help of small pores, but as more particles are trapped, air permeability, another important parameter in filter evaluation, decreases. Therefore, a new filtering mechanism, electrostatic filtration, has developed for the collection of particles with any size. Its principle depends on the electrostatic forces occurred between electrically charged particle and electrically opposite charged filter material. In this

way, it has been shown that electrical and chemical forces can be utilized to capture PM in a proactive manner (Wang and Otani, 2013). The efficiency of the filter depends on the air velocity and the magnitude of the electrical attraction. This principle, which is not preferred in air conditioning systems due to its high investment cost and maintenance, is used in large industrial dust collectors and small portable collectors used to capture particles (Ulutepe, 2007).

High efficiency particulate air (HEPA) and ultra-low particulate air (ULPA) filters used to collect air particles are defined in many standards such as minimum efficiency reporting value (MERV) standard, European Norm (EN 1822) etc (Esteves et al., 2016). These standards are valid for high efficiency filters used in general ventilation and air conditioning systems. Owing to the EN 1822 developed within the scope of European standards, HEPA and ULPA filters have been properly classified. According to this standard, the efficiency of the filters is determined according to the particle size that gives the minimum efficiency at a certain velocity. This size, also called most penetrating particle size (MPPS), is 0.3 μm for HEPA filters. As given in Table 2.3, according to the definition in the EN 1822; HEPA filters are high efficiency air filters with classes ranging from H10 to H14 (Ulutepe, 2007).

Table 2.3 EN 1822 classification for HEPA and ULPA filters (Ulutepe, 2007).

	Filter Class	**Removal efficiency according to MPPS, %**
HEPA	H10	≥ 85
	H11	≥ 95
	H12	≥ 99.5
	H13	≥ 99.95
	H14	≥ 99.995
ULPA	U15	≥ 99.9995
	U16	≥ 99.99995
	U17	≥ 99.999995

2.3 Nanomaterials: Silver nanowire and MXene

The development of nanotechnology enabled production of materials at the nanoscale (nanomaterials) that show unique properties. Nanomaterials classified according to their sizes, have been used frequently in many different applications in recent decades. Within the scope of this thesis, one dimensional (1-D) silver nanowires (Ag NWs) and two dimensional (2-D) MXenes were used.

2.3.1 Silver nanowires (Ag NWs)

Silver (Ag) received great deal of interest by having important properties such as great electrical and thermal conductivity, antibacterial activity, and high mechanical flexibility. Silver nanostructures vary (i.e. beams, particles, tubes, rods and wires etc.) in sizes, shapes and characteristics (Khodashenas and Ghorbani, 2015). Since silver's 1D form, referred to as Ag nanowires (Ag NWs), are defined as 1-D nanomaterials with diameters in the range of 10-200 nm and lengths of 5-100 μm, their aspect ratio is very high (Bahçelioğlu et al., 2019; Zhang et al., 2017). Synthesis methods, fabrication methods and the practical applications of Ag NWs are summarized in Figure 2.2.

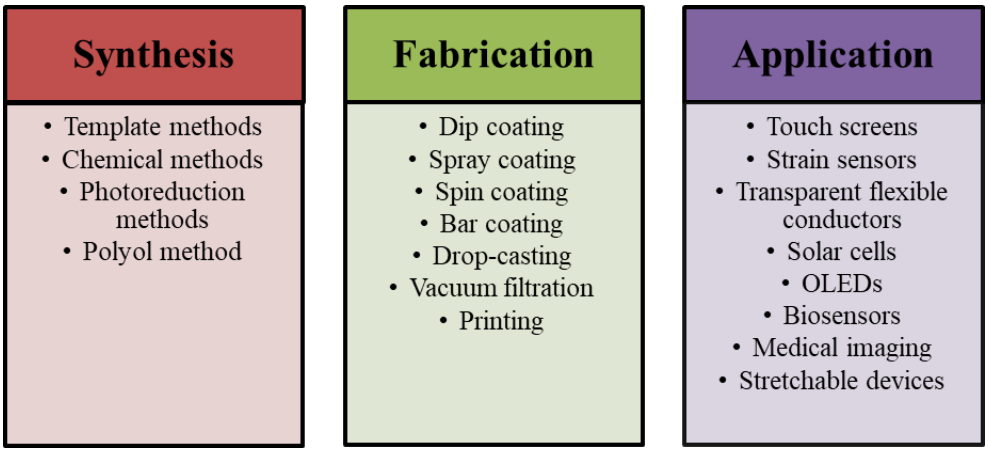

Figure 2.2 Synthesis, fabrication, and applications of Ag NWs.

Several synthesis techniques, mainly divided into template methods, chemical methods, photoreduction, and polyol method are proposed in order to get high-quality, well-formed and high-yield Ag NWs (Fu et al., 2022; Shi et al., 2019).

In the past, Ag NWs were mainly synthesized by electrochemical methods, but the synthesized Ag NWs were not uniform and the synthesis efficiency was not high (Zhang et al., 2017). Therefore, various templates have been developed that provide a specific size and structure in the transformation of nanoparticles into nanowires (karamako, 2000; Kumar et al., 2021). Simple hard template method enables effective production of Ag NWs with controllable morphology and aspect ratio. The common procedure includes preparation of hard templates, functionalization of template, coating the templates with the Ag NW, and purification step (Rodriguez-Abreu et al., 2011). The purification step requires dissolution of the nanoporous support, which often damage the nanowires (Sun et al., 2002). Since this limitation has prompted the development of a new method, soft template methods have emerged. These methods use soluble chemicals in Ag NW production to easily separate the synthesized nanowires from the solvent phase. In order to avoid the template purification step, chemical synthesis techniques (i.e. hydrothermal method, solvothermal method etc,) are also developed for the scalable industrial production of Ag NW (Kumar et al., 2021). As another template-free method, ultraviolet (UV) irradiation, which is a kind of photoreduction method, is developed (Shi et al., 2019).

Among various synthesis routes are disclosed, polyol method and its modified versions are the most promising ones due to their cost effectiveness, mass production capability, simplicity, controllability, and uniformity (Kumar et al., 2021; Zhang et al., 2017). This method is performed by reducing silver salts (i.e. $AgNO_3$) or silver oxides at a high temperatures with polyols (i.e. polyvinylpyrrolidone, PVP) as a template and stabilizing agent. Generally, ethylene glycol (EG) is utilized as both reducing agent and solvent (Coşkun et al., 2011). The factors affecting the synthesis of Ag NWs in the polyol method include reagent concentrations, salt mediator type

and concentration, stabilizing agent concentration and molecular weight, and reaction temperature (Hemmati et al., 2020).

There are many methods used to decorate the synthesized Ag NWs onto various substrates from polymers to fibrous materials. These methods are dip coating, spray coating, spin coating, bar coating, drop-casting, vacuum filtration, and printing. The simplest of these methods is drop casting, which involves dropping a nanowire dispersion onto a substrate and then evaporating the residual solvent (Sohn et al., 2019). Similar to drop casting, dip coating is also a simple and economical method for depositing the nanowire dispersion onto substrate by dipping and then evaporating the residual solvent by drying process (Tang and Yan, 2017). In another technique, called spin coating, nanowire-deposited homogenous and small films are produced and then the residual solvent is evaporated due to the principle of centrifugal force (Zhang et al., 2021). Bar coating, also known as Mayer-rod coating, includes the procedure of the depositing nanowire dispersion to one point of a substrate and sweeping the solution with a Mayer-rod to spread the nanowire dispersion across the substrate (Dong et al., 2015). Spray coating method enables simple, homogeneous, and scalable deposition of multiple layers of nanowires on substrates through a nozzle under the action of compressed gas (Zhang et al., 2021; Sohn et al., 2019). The vacuum filtration, also known as transfer method, is used for constructing homogeneous nanowire network. Practically, it consists of forming a nanowire network by filtering the nanowire dispersion out of residual solvent, and then transferring the network layer to the substrate (Kwon et al., 2018). Recently developed printing technique can also be used to deposit nanowires onto substrates through a cheap, scalable and versatile way. This method has various types including inkjet printing, gravure printing, screen printing, electro-hydrodynamic jet (EHD) printing, roll-to-roll (RTR) printing, and capillary printing.

Ag NWs, which have huge potential for practical applicability in a broad range of technologies such as touch screens, strain sensors, transparent flexible conductors,

solar panels, organic light emitting diodes (OLEDs), biosensors, medical imaging, and stretchable devices, have also started to be used for the environmental purposes such as wastewater treatment, air purification, water purification, desalination, and sensors for water quality monitoring (Bahçelioğlu et al., 2020; Zhang and Hsieh., 2020).

2.3.2 MXene

MXenes, which was discovered by Prof. Yury Gogotsi (Drexel University, USA) and his research group in 2011, are a large family of 2-D materials consisting of transition metal carbides, nitrides, and carbonitrides (Karaman, 2020; Rasool et al., 2019). MXenes have a general formula of $M_{n+1}X_nT_x$, where M represents an early transition metal such as Ti, Sc, Zr, V, Nb, Cr, and Mo, X indicates carbon and/or nitrogen, T denotes termination groups (-OH, -O, or F), n = 1, 2, or 3, and x is the number of terminations (Zhao et al., 2020). With their excellent electrical conductivity, abundant surface functionalities, in-plane stiffness, and scalability, MXenes show a great potential in a variety of applications such as supercapacitors, batteries, portable electronics, hydrogen storage media, photoelectrodes, electromagnetic interference shielding coatings, gas-separation membranes, hydrogen storage media, catalyst supporters, and additives (Lei et al., 2015; Zhao et al., 2020).

Mainly two approaches are utilized in the synthesis of MXenes. In bottom up approach, which includes chemical vapor deposition, template method and plasma enchanced laser deposition, high crystalline quality MXenes are produced without any floride terminations (Verger et al., 2019). In top down approach, MXenes are derived through selectively etching layers of metals from their corresponding three-dimensional (3-D) MAX phase materials with the general formula of $M_{n+1}AX_n$, where A represents A-group element (Karaman, 2020; Rasool et al., 2019). The production mechanism of MXenes from MAX phase materials is shown in chemical

equations, namely, Equation 1, Equation 2, and Equation 3 (Iqbal and Hamdan, 2021):

$$M_{n+1}AX_n + 3HF \rightarrow AF_3 + 3/2\ H_2 + M_{n+1}X_n \quad (1)$$

$$M_{n+1}X_n + 2H_2O \rightarrow M_{n+1}X_n(OH)_2 + H_2 \quad (2)$$

$$M_{n+1}X_n + 2HF \rightarrow M_{n+1}X_nF_2 + H_2 \quad (3)$$

The top down approach consists steps of etching, intercalation and exfoliation. In the etching step, A layer is replaced by termination groups (-OH, -O, or F). Synthesizing MXenes from MAX phase materials can be performed by direct use of hydrogen fluoride (HF) as the etchant or with in-situ HF. In-situ HF is formed by the reaction between hydrochloric acid (HCl) and fluoride salt (i.e. lithium fluoride, LiF) (Rasool et al., 2019). In the intercalation step, an organic solvent such as dimethyl sulfoxide (DMSO) is used to obtain a single or few-layer MXenes (Lei et al., 2015). In the exfoliation step, sonication or shaking is applied to exfoliate the layers (Karaman, 2020).

2.4 Studies conducted on air filtration by Ag NW and MXene

The air purification performance of nanomaterials has improved over the years. Many different filter materials such as polyester, nylon, cotton etc., are developed with nanomaterials such as graphene, silver nanoparticles, nanowires etc., to capture PM. Outstanding studies in the literature on the use nanomaterials in air purification are summarized and presented in Appendix A.

In order to evaluate the performance of the filters, it is necessary to examine some critical parameters, especially the removal efficiency and pressure drop. Removal efficiency defines how well a filter removes airborne particles (Maroto, 2011). Since the pressure drop represents the filter's resistance to air flow, it is important to determine the fan energy needed for the filter.

Since the removal of PM with electrostatic forces is especially effective on small air particles, research on voltage application in filtration systems has increased. PM can be captured with a higher efficiency via electrostatic attraction called “Coulomb force” as described in Equation 4 (Jeong et al., 2017; Zhang and Hsieh, 2020). The mechanism of PM removal by voltage application is explained in Figure 2.3.

$$F_{coulomb} = k_e \frac{q_1 q_2}{r^2} \tag{4}$$

,where, $F_{coulomb}$ is the Coulomb force, k_e represents the Coulomb’s constant, q_1 and q_2 denote the charge on objects, and r is the distance between objects.

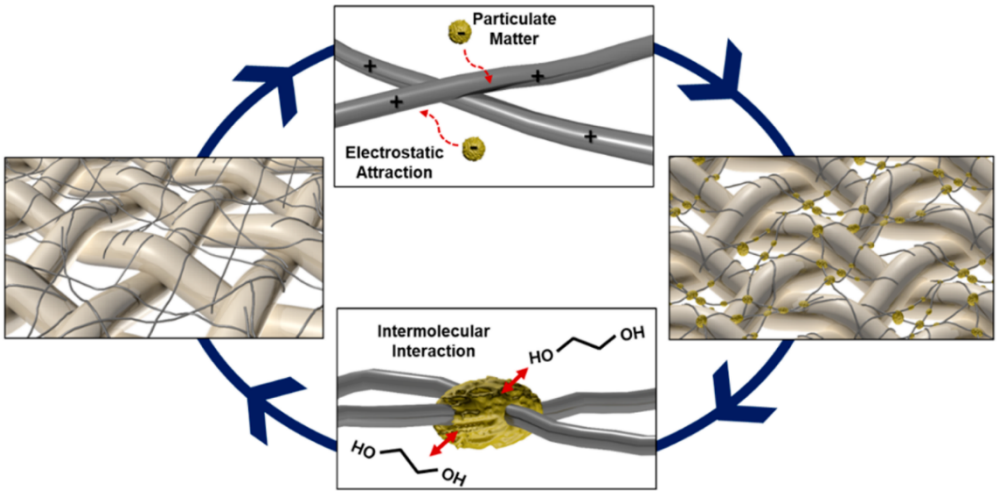

Figure 2.3 A schematic for the PM removal mechanism through conductive nanomaterial coated filters (Jeong et al., 2017).

In the scope of this thesis, Table 2.4 summarizes the results of the studies conducted with Ag NW and MXene in the field of air filtration. These nanomaterials, which were preferred due to their high specific surface areas, are able to capture negatively charged PM thanks to their high electrical conductivity. Besides, they can be decorated onto nylon mesh with large openings, without changing the pore sizes. In this thesis, large area nylon meshes (14 cm x 14 cm) were easily decorated with nanomaterials.

Although there is no study in this field in Turkey yet, the number of studies using Ag NWs in PM removal has increased recently. For example, Jeong et al. (2017) developed, for the first time, a voltage-applied Ag NW-nylon system designed to collect PM by electrostatic forces (Figure 2.3). This type of filtration system has several advantages such as high antibacterial performance and reusability. Then, Huang et al.(2019) designed a flexible, transparent, stable and voltage-applied Ag-nylon mesh for $PM_{2.5}$ removal. The cost of fabrication was reported as $15.03 and fabrication took only 20 minutes. Zhang and Hsieh (2020) designed a simple, low-cost, versatile and scalable electrostatic air filter with the help of Ag NWs and titanium dioxide (TiO_2) nanoparticles for PM removal and formaldehyde decomposition. Lian et al. (2020), proposed a multifunctional electronic textile (e-textile) based on cotton substrates decorated with Ag NWs for different purposes including $PM_{2.5}$ filtration. Park et al. (2021) developed Ag NW coated polyacrylonitrile (PAN) fibres for anti-bioaerosol treatment. In a very recent study, Narakaew et al. (2022) utilized Ag NW bamboo-charcoal composition networks on nylon sheets for PM removal by electrostatic and intermolecular forces.

Compared to Ag-nanomaterial decorated filters, there is limited number of studies (Gao et al., 2019) in the literature on the use of MXene for air filtration. Only Gao et al. (2019) utilized two-dimensional titanium carbide $Ti_3C_2T_x$ MXene nanosheets coated onto PAN nanofibers for $PM_{2.5}$ and bacteria removal. MXene-decorated PAN filters were produced by electrospinning method.

Although the efficiencies in HEPA filters (Table 2.3) are very high, the pressure drops are 25-60 times higher than the drops in Table 2.4 (Zhang and Hsieh, 2020). As seen in Table 2.4, the studies performed with nanomaterial decorated filters led to $PM_{2.5}$ removal efficiencies of 98- 99.99 % with pressure drop range of 3.5-42 Pa. These low pressure drops and obtained mass concentration based-removal efficiencies seem promising; yet, there is still room for improvement, regarding number concentration-based removal efficiency.

Table 2.4 Properties and results of the studies conducted with Ag NW and MXene for PM removal.

Nanomaterial	Result	Reference
Ag NWs	$PM_{2.5}$ removal efficiency: > 99.99 % Pressure drop: 3.51 Pa	Jeong et al. (2017)
Ag NWs	$PM_{2.5}$ removal efficiency: 99.65 % Pressure drop: 14.43 Pa	Huang et al. (2019)
TiO_2 decorated -Ag NWs	$PM_{2.5}$ removal efficiency: 99.5 % Pressure drop: 11 Pa	Zhang and Hsieh, (2020)
Ag NWs	$PM_{2.5}$ removal efficiency: > 98 %	Lian et al. (2020)
Ag NWs	$PM_{2.5}$ removal efficiency: 98.3–99.6 % Pressure drop: 4 Pa	Park et al. (2021)
Ag NWs	$PM_{2.5}$ removal efficiency: > 99.9 %	Narakaew et al. (2022)
MXene	$PM_{2.5}$ removal efficiency: ~99.7 % Pressure drop: ~42 Pa	Gao et al. (2019)

CHAPTER 3

MATERIALS AND METHODS

This chapter covers the materials used in the experiments, methodology of the study, experimental set-ups and procedures, and characterization methods in detail.

3.1 Materials

A nylon mesh with openings of 20 μm × 20 μm was used as filter material in this thesis. Polyvnylpyrrolidone (PVP) (MW = 55,000), ethylene glycol (EG), silver nitrate ($AgNO_3$), and sodium chloride (NaCl) used for Ag NW synthesis were purchased from Sigma-Aldrich. Lithium fluoride (LiF), hydrochloric acid (HCl) used for MXene synthesis were purchased from Sigma Aldrich. For the MAX phase, Ti_3AlC_2 MAX powder (Laizhou Kai Kai Ceramic Material Co. Ltd) was used. Ultra-pure water (18.3 MΩ) used throughout this study was obtained by MilliQ water purification system, Millipore. The electrical resistance of filter was measured with a multimeter (TENMA 72-7730).

3.2 Development methodology of nanomaterial-decorated filters

In order to develop conductive nanomaterial-decorated filters for air purification, several filters were produced. The methodology for production of conductive nanomaterial-decorated filters followed in this thesis is given in Figure 3.1.

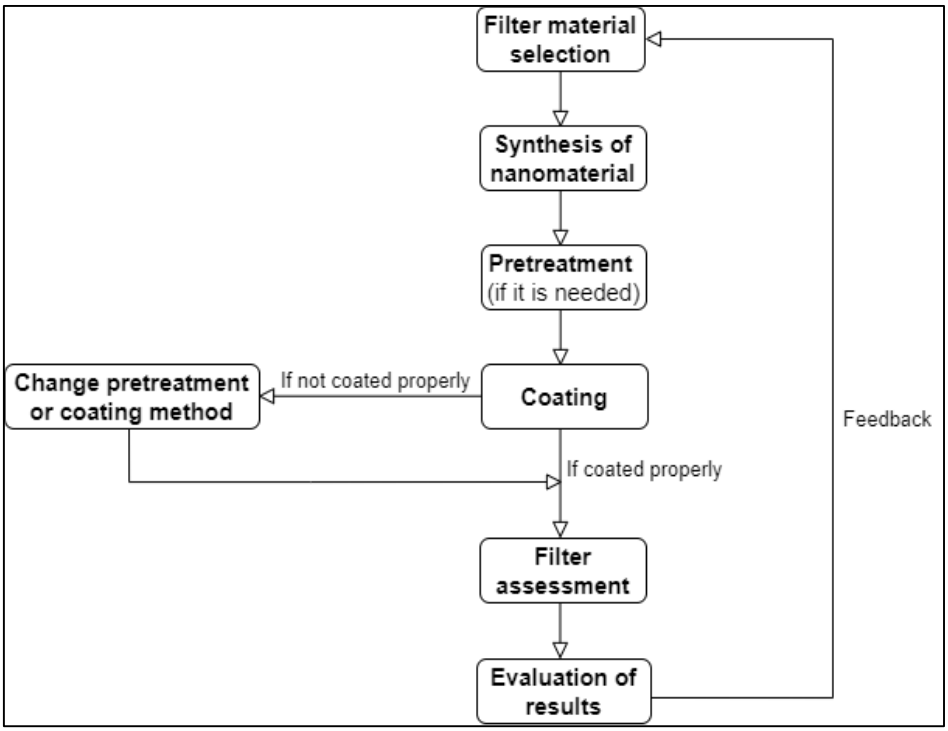

Figure 3.1 Methodology for the production of nanomaterial-decorated filters.

Based on that methodology, nanomaterials were synthesized as a first step. Then, if it is needed, pre-treatment procedures were applied. Filter materials are uniformly coated with the selected nanomaterial. The existence of a proper and uniform coating can be understood by resistance measurements and some characterization routes such as Scanning Electron Microscope (SEM) examination. If the filter material was not coated properly, coating or pre-treatment method was changed. Provided that filter material was coated properly, filter assessment was conducted. Depending on the results of the tests performed to evaluate the performance of developed filters, if required, the filter fabrication part, which consists of filtration material selection, nanomaterials synthesis, pre-treatment of nanomaterial, and coating of filter material, was improved.

3.3 Fabrication of filters

3.3.1 Selection of filtration material

Nylon mesh was chosen as filtration material for specific reasons. Firstly, nylon mesh is an easily accessible and inexpensive material, and can be coated with nanomaterials even though it has large openings. In addition, owing to the voltage application, it comes to a structure that can hold the particles in the air (Jeong et al., 2017; Zhang and Hsieh, 2020). Besides, due to its thin and light structure, it leads to low pressure drops (Huang et al., 2019). Contrary to traditional filter materials, it might show its effect even in a single-layer use (Narakaew et al., 2022).

3.3.2 Synthesis of nanomaterials

Within the scope of this thesis, Ag NWs and MXene were used as conductive nanomaterials. Ag NWs were synthesized by an improved polyol method developed by Coskun et al. (2011). Photos from a typical synthesis cycle is provided in Figure 3.2.

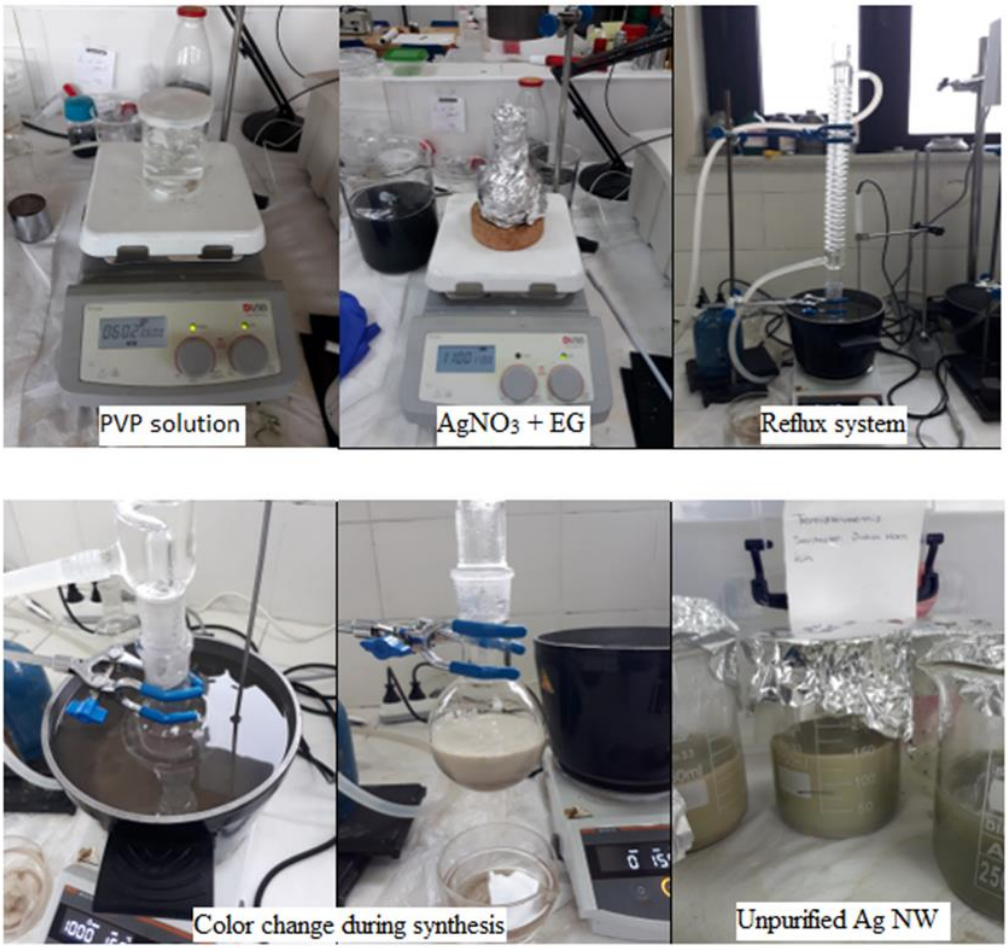

Figure 3.2 Photographs of Ag NW synthesis by polyol method.

Regarding this method, firstly, PVP solution, which was used as a stabilizing agent, was prepared. 1.77 g PVP, 5 mg NaCl, and 80 ml EG were stirred with each other at 800-1000 rpm at 60°C for 20 min. Then, the solution was left for 1 day to become ready for use. 0.68 g $AgNO_3$ and 40 ml EG were mixed at 1000 rpm for 20 min in a way that is not exposed to sunlight. This solution was placed in a hot silicon oil bath that was stirred at 1000 rpm. In here, dropwise addition of PVP solution were performed. The distillation column of the reflux system was fixed to the top of the flask containing the solution and the reaction was started at 160^{o}C for 80 min. Color change to grey indicated formation of Ag NWs. Following synthesis, purification was performed in order to eliminate unwanted by-products such as Ag particles. Purification was conducted through decantation, centrifuging, and multiple times

sedimentation by ethanol. As a result, purified Ag NWs were suspended in ethanol and prepared for later use.

As another nanomaterial used in this study, MXene nanosheets were fabricated through the liquid exfoliation method (Iqbal and Hamdan, 2021). In a typical fabrication method, 3.1 M LiF solution was prepared in 40 ml of 9 M HCl solution in a polytetrafluoroethylene (PTFE) beaker. Then, 2 g of Ti_3AlC_2 MAX powder was added slowly to the prepared solution, and then, the mixture was stirred with 350 rpm at 35°C for 24 h. The resulting products were washed several times using ultra-pure water with centrifugation at 4000 rpm until the pH of the dispersion reaches 6. The delaminated MXene nanosheets were separated from the unreacted MAX phase by centrifugation at 4500 rpm and the fabricated MXene nanosheets were collected from the supernatant. MXene nanosheets from supernatant was concentrated using centrifugation at 10000 rpm for 10 min, and then, the concentration of MXene nanosheets-water dispersion was set to 5 mg/ml for further deposition process and characterizations.

3.3.3 Pre-treatment of filter material

Pre-treatment of filter material was performed for proper coatings. Prior to pre-treatment, nylon mesh was subjected to cleaning procedure to avoid any residue on the filter surface. 14 cm x 14 cm sized nylon mesh was cleaned in an ultrasonic bath using acetone, deionized water, and ethanol for 15 minutes each.

Filtration materials might be both hydrophobic or hydrophilic. Nylon mesh, which is used as filter material in this study, is hydrophobic. However, the thick PVP layer on the walls of Ag NWs synthesized by the polyol process is hydrophilic (Atwa et al. 2015). Therefore, nylon mesh to be coated with Ag NWs must be pretreated to obtain uniform coatings. A modified version of Atwa et al. (2015)'s method (Figure 3.3) was used as the pre-treatment of nylon mesh to be coated with Ag NW. For

MXene-decorated nylon mesh (MDNM) filters, no pre-treatment procedure was used.

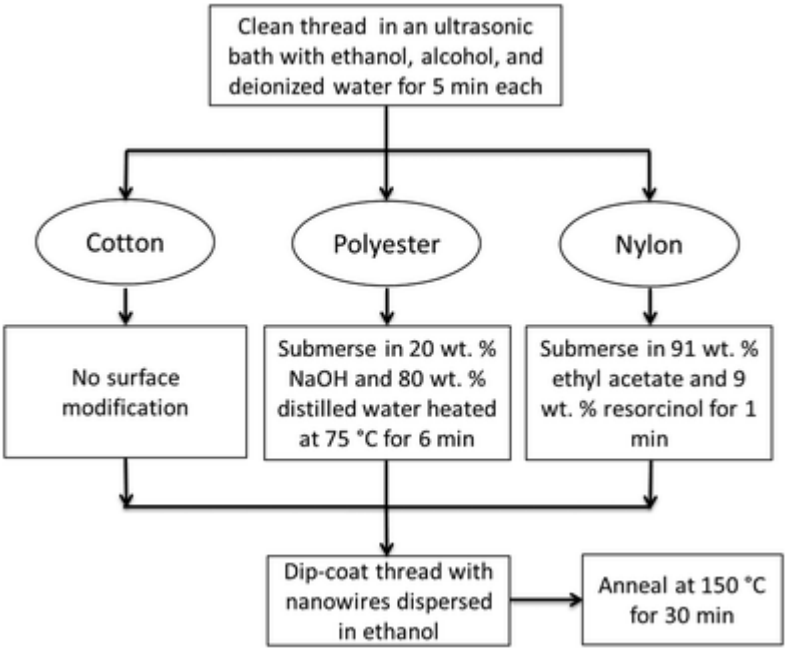

Figure 3.3 Pre-treatment and coating procedure of the filter thread (Atwa et al., 2015).

In original procedure of Atwa et al. (2015) , nylon was submerged in a solution consisting of 91 wt.% ethyl acetate and 9 wt.% resorcinol for 1 minute and then annealed at 150^{o}C for 30 min (Figure 3.3). In this thesis, this procedure was modified via various experiments, which were mentioned in detail in the results and discussion part. These include the modification of the drying temperature, annealing time, and chemical compositions. As a result of these experiments, it was decided that the nylon mesh must be submerged in a solution consisting of 95 wt.% ethyl acetate and 5 wt.% resorcinol for 1 minute and then annealed at 80^{o}C for 10 min.

3.3.4 Coating of filter material with conductive nanomaterial

There are different coating methods used in the decoration of nanomaterials onto filtration materials. The most widely used one is dip coating (Lian et al., 2020; Zhang and Hsieh, 2020; Eom et al., 2017) as schematized in Figure 3.4.

In dip coating method, filtration materials are dipped in nanomaterial dispersion, and then placed into a drying oven. These two processes make one cycle. The duration and temperature of processes depend on the filter material used and the density of nanomaterials in dipping solution. Each cycle was 20 minutes for both coating either with Ag NWs or MXene. The drying process was carried out at 80°C.

The dipping and drying cycles were repeated until the desired resistance values were obtained. The goal at the end of the coating was that the filters have a uniform resistance of 10-100 Ω over the entire surface. Having a resistance in this range is important for the voltage to be applied. As shown in Figure 3.5, in order to ensure voltage application, nearly 1 cm wide silver paste and silver tapes were applied to both sides of the filters.

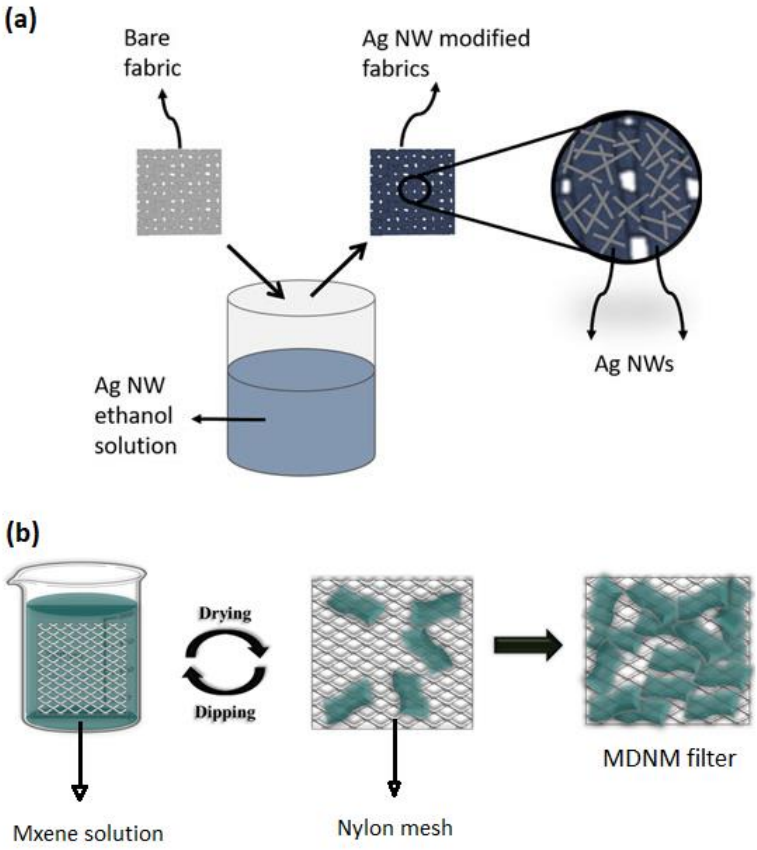

Figure 3.4 Schematic illustrations of dip coating method for (a) Ag NW decoration (Doğanay et al., 2019), (b) MXene decoration.

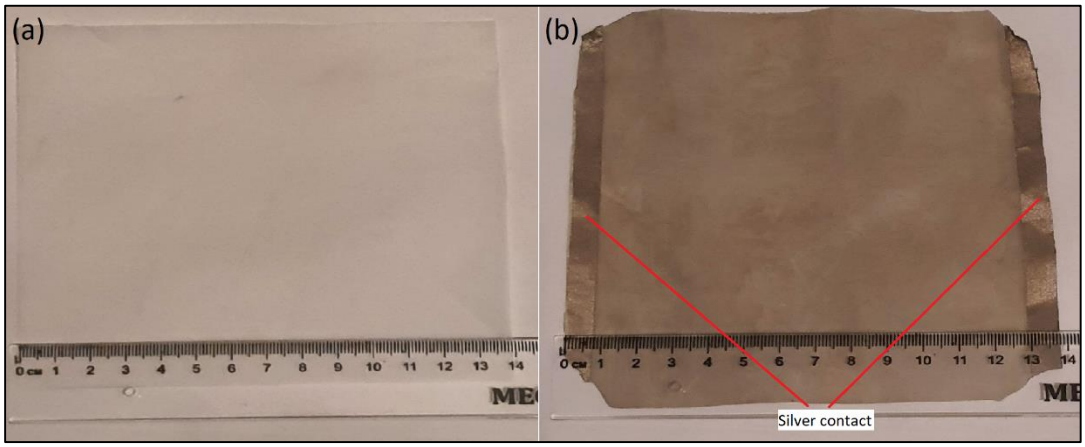

Figure 3.5 (a) Photograph of bare nylon mesh, (b) Photograph of Ag NW-decorated nylon mesh with silver contacts.

3.4 Filter assessment

Filter assessment was conducted to determine the filtration performance of the produced Ag NW-decorated nylon mesh filters and MDNM filters. In order to compare the developed filters' performance, a commercial HEPA filter (AFT Filter, Micro Glassfiber) was also used as a reference. Regarding to EN 1822 standards, this HEPA filter is in the filter class of H13 (Table 2.3) and has a removal efficiency of 99.95% (Appendix B). The filtration set-up used in the filter evaluation tests, the content of the evaluation tests, and the details of the characterization tests are given in the following sections.

3.4.1 Filtration set-up and operation

Several experiments were performed to determine filtration efficiencies of Ag NW-decorated nylon mesh filters and MDNM filters. Filtration tests had to be carried out in an airtight set-up and in a steady environment. Therefore, a filtration set-up was designed and in-house fabricated. A schematic illustration of the filtration set-up is shown in Figure 3.6. This set-up was designed to test both conductive nanomaterial-decorated filters and HEPA filter. All the filtration tests were performed in a calm and steady room.

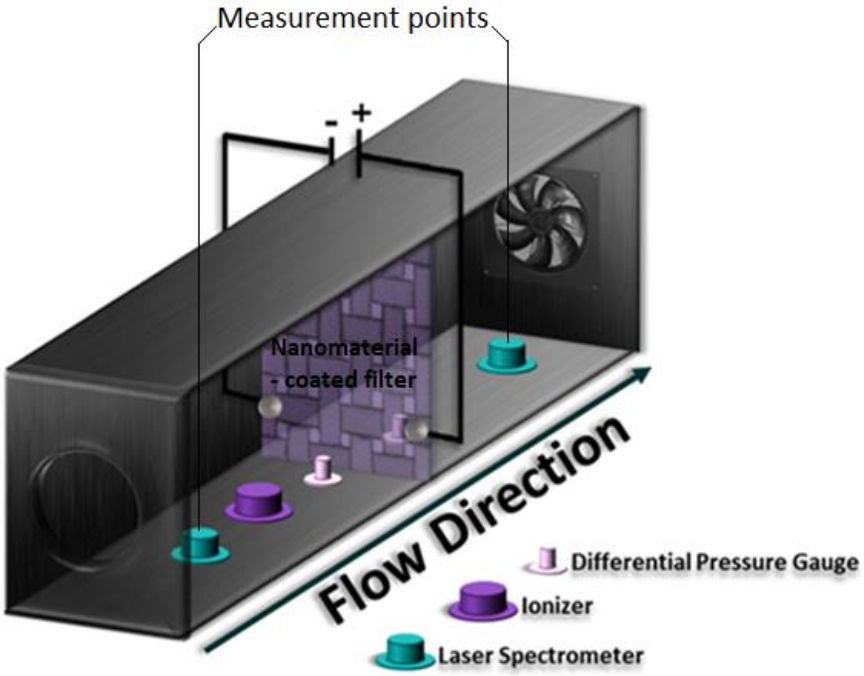

Figure 3.6 Schematic illustration of the filtration set-up fabricated in this work.

As shown in Figure 3.7, the experimental set-up contains two divided plexiglass chambers, consisting of a fan, particle counter, power supply, pressure gauge, and ionizer. The conductive nanomaterial-decorated nylon mesh filter was fixed in the middle of the two chambers via a plexiglass frame. In this way, the filters could be easily changed without changing the air tightness of the set-up. A fan (Taida-Tidar) was installed to provide sufficient air flow to the set-up. Most of the studies performed with different air filtration materials, utilize an additional PM source such as burning incense, in order to simulate a polluted environment (Jeong et al., 2017; Jung et al., 2018; Narakaew et al.,2022). In this study, without using an extra PM source, the indoor air was drawn by a fan. At the inlet part of the chamber, an ionizer (TRUMPXP, TFB-YD1249) was located to negatively charge PM. The particles in both chambers were counted via Laser Aerosol Spectrometry (LAS) device called Grimm Environmental Dust Monitor (EDM) 107. An anemometer (ALMEMO, 2290-4) was used for measuring the airflow velocity. A power supply (TT TECHNIC MCH305D-II) served two purposes: applying voltage and changing fan speed. A

digital differential pressure manometer (CEM, DT-8890) was used to detect the pressure drop during filtration.

Grimm EDM 107 has options to save data with intervals such as 6 seconds, 1 minute, and 5 minutes etc. For this study, this interval was adjusted to 1 minute. Since there is only one particle counter for this study, the inlet PM measurement was performed when the air at the inlet measurement point of set-up becomes stable, and then PM measurements were performed at the outlet measurement point of the set-up.

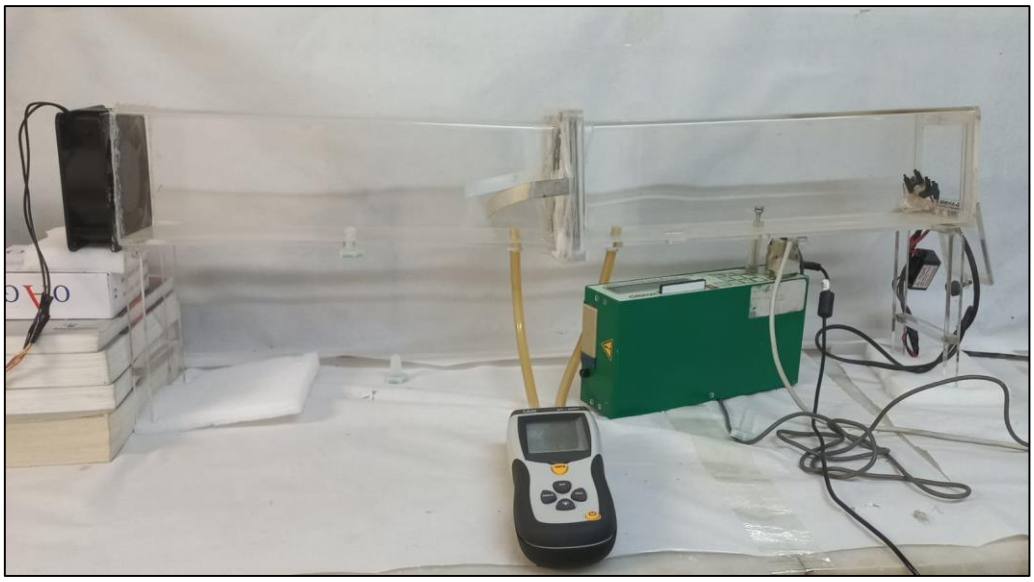

Figure 3.7 Photograph of the filtration set-up.

3.4.2 Filter evaluation tests

Particularly in their practical application, there are some critical parameters that must be provided to evaluate the performance of filters. Among these parameters, removal efficiency is regarded as the most important one. Following the removal efficiency, air permeability is also considered as an important parameter, which is expressed by the term pressure drop. Filtration materials with multifunctional performance such as reusability have received attention with the increasing demand for effective air filtration applications (Liu et al., 2020). Therefore, the effect of voltage application,

the effect of air velocity, the effect of repeatability, the effect of reusability, and the effect of 2-hour filtration performance on these two parameters, namely, removal efficiency and pressure drop, were investigated. To this purpose, for all experiments, the same filtration test set-up was used, yet either with different filters, or voltage applications, or air velocities, etc. All filtration tests performed for each effect were repeated 5 times for both filter types, i.e., Ag NW decorated-filters and MDNM filters. In all experiments, indoor air that is entering the inlet chamber and filtered air at the outlet chamber were analyzed for the calculation of PM removal efficiency. Pressure drop was also monitored for each test performed.

3.4.2.1 Voltage application

In this study, the nanomaterial-decorated filters were investigated in the improvement of indoor air quality. With the collaboration of nylon mesh, nanomaterial-decorated filters were expected to show a promising performance in PM removal, owing to their high electrical conductivity and large surface area. Different procedures were applied to the filters to determine the effect of voltage and ionizer on PM removal. Voltage was applied to the right and left parts of the silver paste-coated parts of filters. It was predicted that a strong electrostatic attraction force would formed between positively charged nanomaterial-decorated filters and negatively charged particles with the help of the ionizer.

In this step, air velocity was adjusted to 1.02 m/s for two reasons. Firstly, it was the maximum speed the fan used in this study could reach. Secondly, since other studies in the literature (Han et al., 2021b; Jeong et al., 2017; Zhang and Hsieh, 2020) work with smaller filtration set-ups and proportionally smaller air speeds, it was predicted that lower air velocity would not be sufficient for the 80-cm long set-up used in this thesis. A fan that can give the highest air speed that fits the dimensions of the system was used.

The applied voltages were chosen in parallel with the recent studies in literature (Jeong et al., 2017; Huang et al., 2019; Narakaew et al., 2022). For Ag NW-decorated nylon mesh filters, ionizer (5 V), and ionizer (5 V) with the voltage application of 2.5 V, 5 V, 7.5 V, or 10 V were applied, respectively. For MDNM filters 5 V and 10 V were applied, respectively. Since the nylon could not handle 20 V, the current dramatically disappeared and ruptures occurred on the filter material surface. Thus, the surface of nanomaterial-decorated nylon mesh was heated up through voltage application. This mechanism is known as Joule heating. Therefore, it was decided to apply a maximum voltage of 10 V to the filters. The current generated by applying voltage on MXene was lower. Because a difference of 2.5 V among the voltages studied just slightly changed the current generated on the MDNM filter. A wider voltage range (5 V, 10 V) was studied for MDNM filter.

3.4.2.2 Air velocity

Air permeability, which has an important role in filter performance, indicates the rate of flow of a fluid through a porous material (Zhu et al., 2015). The term pressure drop is used as a measure of permeability, and it is described as the resistance of filter to airflow (Han et al., 2021a; Liu et al., 2020). As the filter gets clogged and its permeability decreases, the resistance of the filter increases, and thus the pressure drop increases.

Filtration performance of air filters varies with air velocity and thus with the air flowrate (Bingbing et al., 2013). Thus, removal efficiencies and pressure drops of the produced filters were tested at two different air velocities of 0.45 m/s and 1.02 m/s. These velocities were obtained by changing the supplied voltage to the fan. A digital differential pressure manometer was used to measure pressure drop of the filter while an anemometer was used to measure the air velocity.

3.4.2.3 Repeatability of nanomaterial-decorated filter production

It is important to produce conductive nanomaterial-decorated filters easily and reproducibly. The repeatability criterion used here is that the filters, which are produced in the same procedure, should have similar characteristics (i.e. conductivity), removal efficiencies, and pressure drops. Therefore, firstly, three identical filters were decorated under the same conditions until similar resistances were obtained. In order to determine their similarity to each other, resistances were measured with a multimeter. Then, the filter performance of each filter was analyzed under the same conditions. These conditions were 10 V of applied voltage and 1.02 m/s of air velocity, which were determined considering the previous studies on this thesis where the highest filtration performance was achieved (Section 3.4.2.1 and Section 3.4.2.2).

3.4.2.4 Reusability

The need to replace or clean a filter when it becomes clogged with particles makes reuse of filtering materials extremely important. The reusability process of filters should be easy, inexpensive, and environmentally friendly. In order to examine the reusability of the conductive nanomaterial-decorated nylon mesh filters, polar solvent washing method was performed (Jeong et al., 2017; Narakaew et al., 2022; Zhang and Hsieh, 2020). Decorated-filters were firstly immersed in an EG solution for 30 seconds, rinsed with ethanol, and then dried at 65^{o}C for 10 minutes. The particles captured by the filter are expected to dissolve in the solvent by strong dipole–dipole interactions caused by strong intermolecular forces (Jeong et al., 2017). At the end of the reusability test procedure, the washed filter was expected to be used repeatedly for air filtration. Thus, after drying, the washed filters were placed in the set-up and filtration tests were applied repeatedly at the predetermined optimum voltage (10 V) and air velocity (1.02 m/s), where the highest filtration

performance was achieved in the previous studies on this thesis (Section 3.4.2.1 and Section 3.4.2.2).

3.4.2.5 2-hour filtration performance

Commercially available filters with surface-particle interaction mechanism are widely used in public places such as hospitals, shopping malls, transportation vehicles, where it is necessary to use the filter without replacement for a long time. At the same time, prolonged exposure to air pollution can lead to a wide variety of health problems and environmental effects. Most air purifiers reduce significant number of airborne pollutants in 1-2 hours (Grinshpun et al., 2005; Cooper et al., 2021; Guo et al., 2021). Thus, the performance of developed filters was tested for 2 hours under predetermined optimum voltage (10 V) and air velocity (1.02 m/s).

3.4.3 Filter characterization

Many methods have been carried out to characterize filters decorated with nanomaterials. For investigating the morphology and chemical content characterization at the filter material surface, SEM and Energy Dispersive Spectroscopy (EDS) analyses were conducted by using FE-SEM (Nova NanoSEM 430) in METU, Department of Metallurgical and Materials Engineering. The elemental maps of the produced filters were obtained at an operating voltage of 10 kV. Fourier Transform Infrared Spectrophotometry (FT-IR) (Bruker IFS 66/S) of METU Central Laboratory was used to monitor the bond change of filters decorated with conductive nanomaterials during the polar solvent wash procedure.

Filter characterization tests were performed both in the fabrication of filters and the filter evaluation tests.

3.5 Calculations of removal efficiency

Filter evaluation tests were carried out to determine some critical parameters in the investigation of filter performance. In order to specify removal efficiency, which is considered as the most critical parameter, the amount of particles in the air before and after the filtration must be known. In this study, airborne particles in the measurement points of filtration set-up were measured by light scattering principle of Grimm EDM 107. In this method, which is approved by USEPA, the intensity of scattering light signal is given in a certain particle size distribution between 0.25 μm and 32 μm from 31 different channels (Grimm Aerosol Technik, 2019). The thresholds of Grimm EDM 107 channels are provided in Figure 3.8. Based on these values, data from the channels were grouped as PM_1, $PM_{2.5}$, and PM_{10}. Removal efficiency calculations were performed for particles from 0.3 μm to 10 μm, because the most penetrating particle size (MPPS) is specified as 0.3 μm in the efficiency tests of HEPA filters according to the EN1822 standard. Since the purpose of this study was to develop a filter, these ranges were studied in order to compare the developed filter with other filters. However, since PM_1 has very important health effects, PM_1 removal efficiencies of the both type of filters (Ag NW- decorated filter and MDNM filter) under optimum conditions are given in Appendix C.

Particulate Matter	Particle size		PM classification
	0.25	0.50	PM_1
	0.28	0.58	
	0.30	0.65	
	0.35	0.70	
	0.40	0.80	
	0.45	1.0	
	1.3	2.0	$PM_{2.5}$
	1.6	2.5	
	3.0	6.5	
	3.5	7.5	
	4.0	8.0	
	5.0	10.0	PM_{10}
	12.5	25.0	
	15.0	30.0	
	17.5	32.0	
	20.0		

Figure 3.8 Thresholds (µm) and classification of Grimm EDM 107 channels.

There are two ways to measure the amount of PM in the atmosphere: mass concentrations and number concentrations. PM counter, Grimm EDM107, used in this study gives the data in count distribution mode (number concentration), which indicates the number of particle concentrations per liter for all particle measuring channels. An example of raw data from Grimm is provided in Appendix D. However, mass concentration is more usually used to indicate PM levels, since current standards are based on mass concentrations. When the amount of particles is converted to mass concentration, it is based on two assumptions used in most particle sizing techniques. Accordingly, it it assumed that all particles have uniform density and spherical shape.

The relationship between the mass concentration and number concentration can be expressed as (Equation 5):

$$m_{dp_i} = C_f \frac{\pi}{6} {dp_i}^3 n_{dp_i} \quad (5)$$

,where *i* denotes channel number of the particle counter; d_{pi} is the arithmetic mean diameter of the upper and lower boundaries for channel i; m_{dpi} is the mass concentration in channel i; n_{dpi} is the number concentration in channel i; and C_f is a correction factor (Cheng and Lin, 2010). Number concentrations were converted into mass concentrations by using an instrument-specific factor (*Cf*) developed by the manufacturer.

Number concentration-based removal efficiency calculations were performed by using Equation 6.

$$\text{Removal efficiency (\%)} = \left(\frac{N_0 - N_1}{N_0}\right) x\ 100\ \% \quad (6)$$

, where N_0 (number of particles / liter) and N_1 (number of particles / liter) denote the number of PM in all sizes at the inlet and outlet measurement points of filtration set-up, respectively.

Mass concentration-based removal efficiency calculations were performed by using Equation 7.

$$\text{Removal efficiency (\%)} = \left(\frac{C_0 - C_1}{C_0}\right) x\ 100\ \% \quad (7)$$

, where C_0 (μg/m^3) and C_1 (μg/m^3) denote the mass of PM in all sizes at the inlet and outlet measurement points of filtration set-up, respectively.

CHAPTER 4

RESULTS AND DISCUSSION

The results obtained from the filtration tests were discussed in this chapter as two main parts: evaluation of the pre-treatment method used in the fabrication of the Ag NW-decorated filters and filter evaluation tests. The results of the characterization tests were also presented here.

4.1 The results of the pre-treatment method used in the decoration of nylon mesh with Ag NW

Photos of bare, Ag NW-decorated or MDNM filters that are produced via dip and dry method are provided in Figure 4.1 (left to right), respectively. For both conductive nanomaterial-decorated filter types, it was possible to achieve a conductive network within usually 20 dipping and drying cycles. The aim was to coat the filters quickly, simply and uniformly. Therefore, it was important to reach the first cycle in which the resistance occurs and the cycle in which the desired resistance (50 Ω) was observed in a short time.

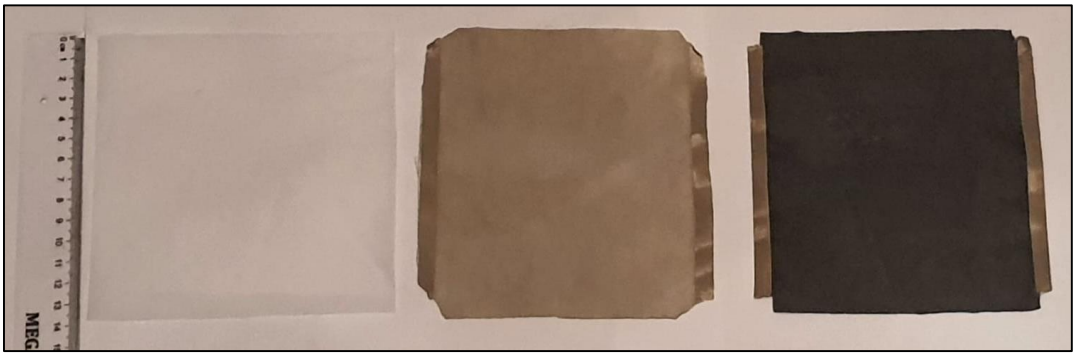

Figure 4.1 Photograph (from left to right) of bare nylon mesh, Ag NW-decorated nylon mesh, and MDNM.

As it was mentioned in Section 3.3.3, Atwa et al. (2015)'s method for coating nylon mesh with Ag NW was used in this thesis study with modifications in annealing time, drying temperature, and chemical percentages. The summary of modifications done and the dipping and drying cycles where the first and the desired resistances were obtained are given in Table 4.1.

Table 4.1 Modification of Atwa et al.'s (2015) pre-treatment procedure.

$wt_{Resorcinol}$(%)	$wt_{Ethyl\ acetate}$(%)	Annealing time (min)	Drying temperature (°C)	1st resistance	Desired resistance
9	91	30	150	-	-
9	91	10	120	8.cycle	27.cycle
9	91	10	80	9.cycle	20.cycle
20	80	10	80	8.cycle	22.cycle
1	99	10	80	7.cycle	23.cycle
5	95	10	80	2.cycle	8.cycle

For the nylon based materials, attaching polar groups such as resorcinol to the surface is a common pre-treatment that increases the hydrophilicity (Atwa et al., 2015). Owing to the hydroxy groups formed on the nylon surface by resorcinol, Ag NWs could adhere to the surface of the nylon mesh more easily and homogeneously. Since the temperature used in Atwa et al. (2015)'s study (150°C) was predicted to damage the nylon mesh, the temperature was first reduced to 120°C, then to 80°C. It was observed that the process at 80°C helped the decoration to take place faster in a shorter time.

The weight percents of resorcinol and ethyl acetate were also changed to observe the effect of the amount of chemical used on the coating of nylon mesh with Ag NW. As a result, it was observed that nylon mesh dried at 80°C using 5 wt.% resorcinol and 95 wt.% ethyl acetate both helped to quickly reach the desired resistance. In

addition, this procedure helped to achieve uniform Ag NW coating on the nylon mesh, as shown in Figure 4.2.

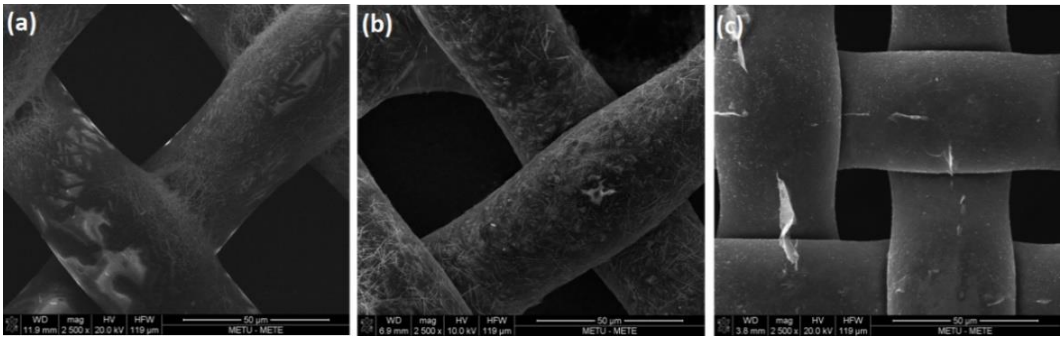

Figure 4.2 SEM images of (a) Ag NW-decorated nylon mesh without any pre-treatment, (b) Ag NW-decorated nylon mesh with a pre-treatment, and (c) MDNM.

4.2 Particles in indoor air

This study assumed that there was no significant change in the indoor air, due to the fact that the laboratory used for filtration tests was specifically arranged for this thesis study. Indoor air was not disturbed by any other means and all filtration tests were performed under similar conditions by using actual indoor air. A PM-producing source was not used. Yet, particle size distribution can influence the actual efficiency, especially, when the particle size distributions are different at different concentration levels. Size distribution of the particles in indoor air during all filtration tests performed in this thesis study are given in Figure 4.3. The particle size-based percentages of indoor air particles are given in Table 4.2.

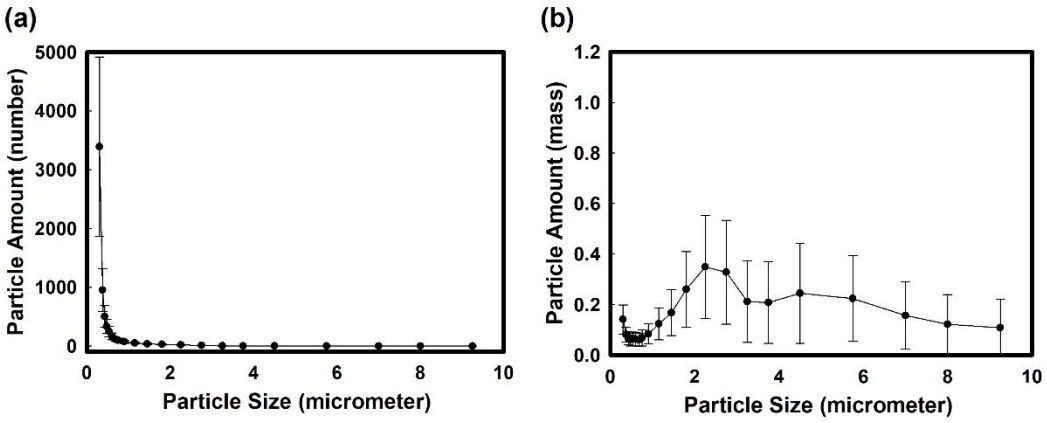

Figure 4.3 (a) Size distribution according to the number concentration of the particles in indoor air, (b) Size distribution according to the mass number concentration of the particles in indoor air.

As seen in Figure 4.3, although the number of small particles such as PM_1 was larger than particles with diameters greater than 1 μm, the bigger particles dominate the mass distribution. Because large particles have larger diameters and thus larger masses.

As seen in Table 4.2, the distribution of the particles and the abundancy of the different-sized particles in the influent air entering the filtration set-up for identical filters were close to each other throughout the filtration tests. As expected, there was no major change in the size distribution of the particles in the indoor air where the experiments were performed.

Table 4.2 Particle size-based percantages of indoor air particles.

Particle size, μm	Abundancy, %	
	Number concentration	**Mass concentration**
0.33	48.72 ± 9.41	5.23 ± 3.55
0.38	17.82 ± 2.38	2.72 ± 1.36
0.43	10.03 ± 1.88	2.17 ± 0.95
0.48	6.63 ± 1.39	1.95 ± 0.75
0.54	4.83 ± 1.08	2.07 ± 0.74
0.62	3.23 ± 0.84	2.01 ± 0.64
0.68	2.32 ± 0.69	1.89 ± 0.57
0.75	1.93 ± 0.61	2.13 ± 0.62
0.90	1.40 ± 0.50	2.63 ± 0.73
1.15	1.01 ± 0.41	3.89 ± 1.04
1.45	0.70 ± 0.32	5.30 ± 1.32
1.80	0.58 ± 0.29	8.22 ± 2.17
2.25	0.40 ± 0.21	11.06 ± 3.07
2.75	0.20 ± 0.11	9.97 ± 2.27
3.25	0.08 ± 0.06	5.85 ± 2.24
3.75	0.05 ± 0.05	5.89 ± 2.37
4.50	0.04 ± 0.03	6.96 ± 3.00
5.75	0.02 ± 0.01	6.80 ± 2.90
7.00	0.01 ± 0.01	5.02 ± 3.60
8.00	0.00 ± 0.00	4.27 ± 3.42
9.25	0.00 ± 0.00	3.96 ± 3.62

In this thesis, conductive nanomaterial-decorated nylon mesh filters were developed to improve indoor air quality with PM filtration. SEM image of a PM captured by the filter is given in Figure 4.4. Determining the elemental composition in fine and coarse particles is important in terms of determining the relationship between particulate matter and human health and the sources of particulate matter. The elemental composition of a sample PM was investigated by EDS analysis, the results of which are provided in Table 4.3. According to this table, the particles in the room where the filtration tests were performed, contain the highest percentage of carbon element by weight, as expected (Taner, 2012). It was also observed that metals such as Al, Si, K, and Ca were present in the PM sample as earth crust elements.

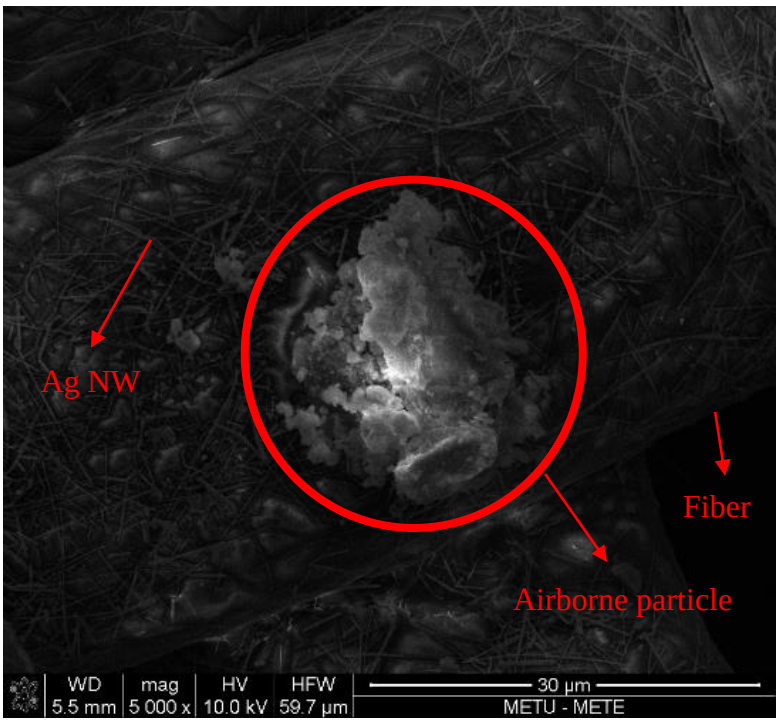

Figure 4.4 SEM image of PM captured by Ag NW-decorated nylon mesh filters.

Table 4.3 Elemental composition of a sample PM.

Element symbol	Weight (%)
C	66.70
O	12.34
Na	2.01
Al	0.91
Si	2.09
S	0.63
Cl	4.04
Ag	6.90
Ca	4.39
Total	100.00

4.3 The results of the filter evaluation tests

4.3.1 The effect of voltage application on the filtration performance of nanomaterial-decorated filters

The effect of the ionizer and the applied voltage on the filtration performance of nanomaterial-decorated nylon mesh filter was verified by filter evaluation tests at different voltage applications. For Ag NW-decorated filters, filtration tests of (i) bare nylon mesh, (ii) only filter, (iii) ionizer with filter, (iv) ionizer with filter (2.5 V), (v) ionizer with filter (5 V), (vi) ionizer with filter (7.5 V), (vii) ionizer with filter (10 V), and (viii) H13 class HEPA filter, were performed respectively. For MDNM filters, tests of (i) bare nylon mesh, (ii) only filter, (iii) ionizer with filter, (iv) ionizer with filter (5 V), (v) ionizer with filter (10 V), and (vi) H13 class HEPA filter, were performed respectively. Each filtration test performed for the cases given in Figure 4.5 and Figure 4.6, was repeated 5 times for both types, namely, Ag NW decorated-

filters and MDNM filters. All figures presented reveal the average and standard deviations of these tests.

Bare nylon mesh had a mass concentration-based removal efficiency of 37.07% and 50.04% for $PM_{2.5}$ and PM_{10}, respectively. It had 15.65% and 15.74% number concentration-based removal efficiencies for $PM_{2.5}$ and PM_{10}, respectively. As seen in Figure 4.5 and Figure 4.6, coating with conductive nanomaterial increase the filtration efficiency of nylon mesh. Compared to the nanomaterial-decorated filters, running the ionizer alone improved the PM removal further (Figure 4.5 and Figure 4.6). Because Ag NW and MXene have good electrical conductivity, as well as high specific surface area, the removal efficiency was greatly enhanced, probably through a strong interaction occurred between accessible surface terminating groups of positively charged nylon mesh filters and negatively charged particles. It has been also observed that increasing voltage increases the removal efficiency, especially in small particles (Figure 4.5 and Figure 4.6). However, a maximum voltage of 10 V could have been applied to the filters in order not to damage the filter material and increase energy consumption. Through a process known as Joule heating, high voltages transform more electrical energy into heat. This caused damages of the surface on nylon mesh.

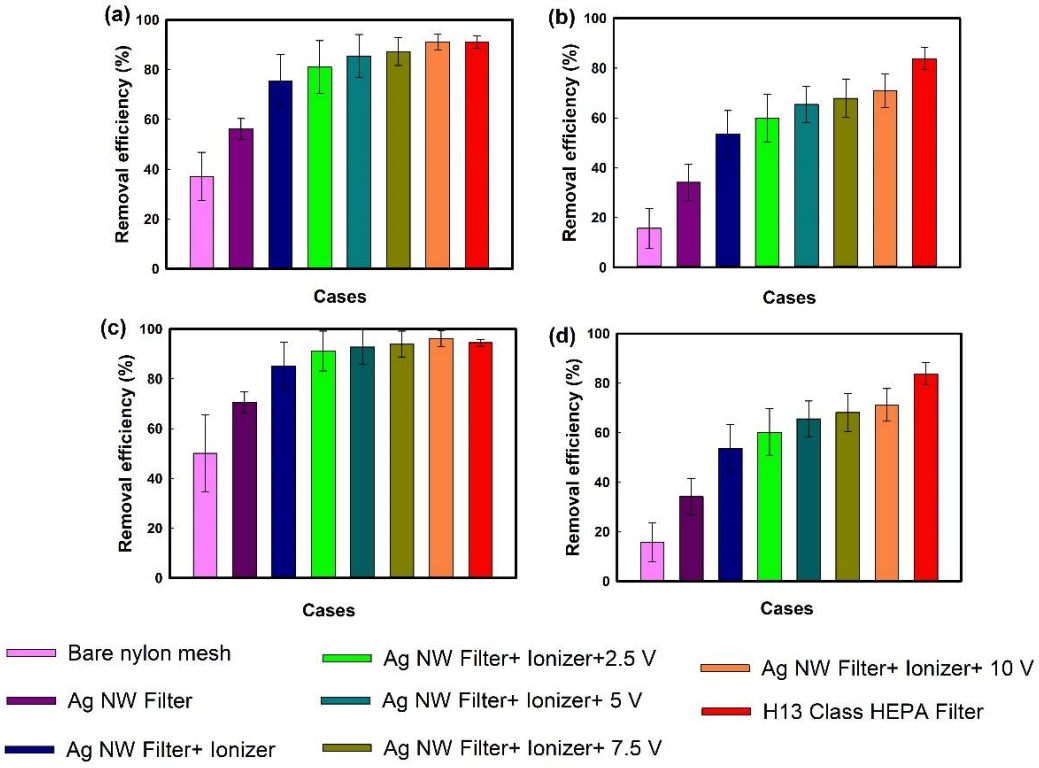

Figure 4.5 $PM_{2.5}$ removal efficiencies of Ag NW-decorated filters based on (a) mass concentration, and (b) number concentration; PM_{10} removal efficiencies of Ag NW-decorated filters based on (a) mass concentration, and (d) number concentration.

For Ag NW-decorated filters, case (vii) demonstrated the best PM removal performance in both mass concentration-based removal efficiency and number concentration based-removal efficiency (Figure 4.5). When the ionizer was on and the applied voltage on the Ag NW-decorated filter was adjusted to 10 V (Figure 4.5 (a) and (c)), Ag NW- decorated filters reached removal efficiencies of 90.98% and 96.11% for $PM_{2.5}$ and PM_{10}, respectively. According to number concentration-based removal efficiency calculations provided in Figure 4.5 (b) and (d), Ag NW-decorated filters reached removal efficiencies of 70.98% and 71.21% for $PM_{2.5}$ and PM_{10}, respectively.

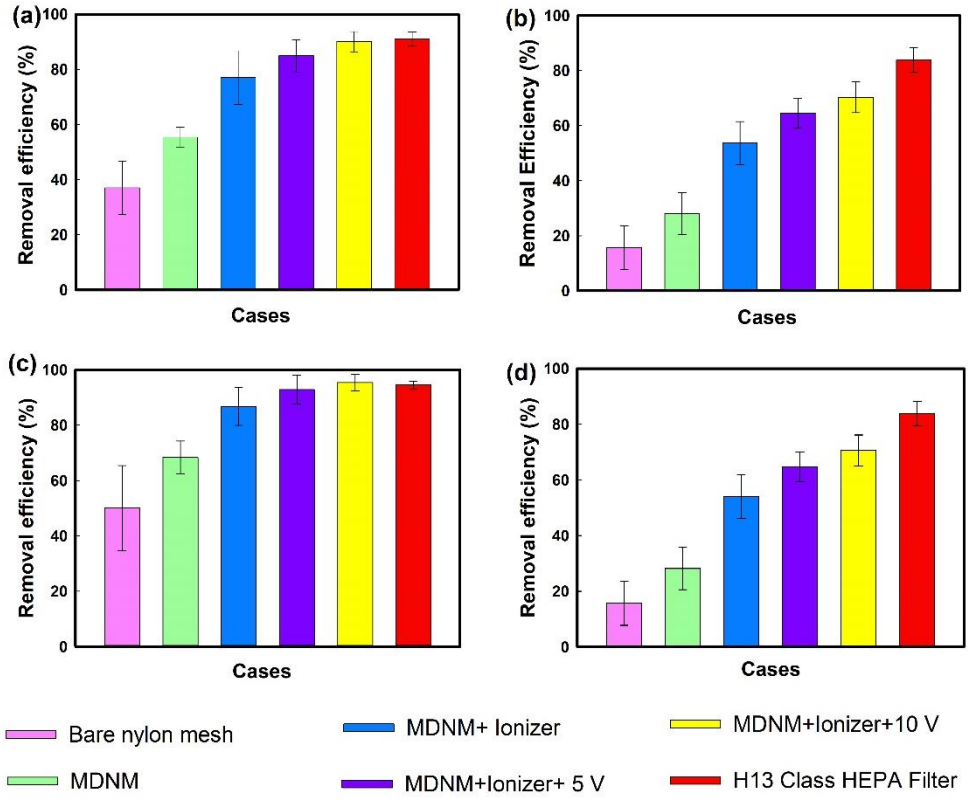

Figure 4.6 $PM_{2.5}$ removal efficiencies of MDNM filters based on (a) mass concentration, and (b) number concentration; (c) PM_{10} removal efficiencies of MDNM filters based on (c) mass concentration, and (d) number concentration.

For MDNM filters, case (v) demonstrated the best PM removal performance in both mass concentration-based removal efficiency and number concentration based-removal efficiency (Figure 4.6). When the ionizer was on and the applied voltage on the MDNM filter was set to 10 V (Figure 4.6 (a) and (c)), MDNM filters reached removal efficiencies of 90.05% and 95.44% for $PM_{2.5}$ and PM_{10}, respectively. According to number concentration-based removal efficiency calculations, MDNM filters reached removal efficiencies of 70.37% and 70.58% for $PM_{2.5}$ and PM_{10}, respectively.

In parallellism with the other studies in literature, the highest mass concentration based-removal efficiency was obtained in this study when the ionizer was on and the

voltage on the filter was 10 V. These results also supported the other studies in the literature. Jeong et al. (2017), Huang et al. (2019), and Narakaew et al. (2022) had the highest mass concentration-based removal efficiency (99.99%, 99.65%, and 99.9%, respectively) when they applied 10 V to their Ag NW decorated-nylon (Table 2.4). However, Zhang and Hsieh (2020) used a voltage as high as 1000 V in their study, where they used polyester as filter material. They also pointed out that the applied voltage for their Ag/TiO_2-polyester filter is even lower than that for other typical electrostatic filters, such as those used by Li et al. (2018), Choi et al. (2017), and Kim et al. (2018), which are 2000 V, 10,000 V, and 20.000 V, respectively (Huang et al., 2019). However, the applied voltage increases energy use and increases cost as well.

According to mass concentration-based removal efficiency calculations, H13 class HEPA filter reached removal efficiencies of 91.03% and 94.51% for $PM_{2.5}$ and PM_{10}, respectively, when it was used in the same filtration set-up at same operation conditions (Figure 4.5). According to number concentration-based removal efficiency calculations, H13 class HEPA filter reached removal efficiencies of 83.81% and 83.84% for $PM_{2.5}$ and PM_{10}, respectively (Figure 4.6). However, based on the EN1822 standards, this HEPA filter must have a mass concentration-based removal efficiency of 99.95% for $PM_{2.5}$ (Appendix B). This difference was also valid for the developed filters and the obtained removal efficiencies of nanomaterial-decorated filters were lower than those in the literature (Table 2.4). This difference might be due to the use of a single particle counter while performing the filtration tests as well as the used filtration set-up. In addition, use of different PM measurement devices, different PM size distribution, flowrate of ambient air, nanomaterial decoration efficiency, nanomaterial characteristics, pore sizes of the filter material, and type of filter material might be used to explain those differences observed in removal performances. Nevertheless, filtration tests also confirmed that, regarding the mass concentration-based removal efficiency calculation values, the conductive nanomaterial-decorated nylon mesh filters have very similar efficiency

to HEPA filters under the same conditions using the filtration set-up. Thus, in this respect, nanomaterial-decorated filters might compete with HEPA filters. However, the applied energy and cost must also be taken into account. HEPA filters require powerful pumps to generate sufficient airflow against high pressure drop across the filter. This can be expensive and energy-intensive. The produced nanomaterial-decorated filters showed low pressure drop during filtration tests, thus they do not need powerful pumps to operate. The production cost of nanomaterial-decorated filters was low. However, it is known that the usage time of the filters and the energy they will consume will affect the operational cost. Therefore, different studies are needed to make a detailed comparison. Also, conductive nanomaterial-decorated filters need to be improved, regarding the number concentration-based removal efficiency.

Mass and number concentrations must be used together when analyzing the results of the filtration tests. The uncertainties were taken into consideration as mass concentrations were computed from the number concentration measurements. Since PM is a mixture with various size distributions, when calculating the total mass of particles below a certain size, it should be taken into account that the particle mass increases with diameter. Thus, the total mass is primarily determined by larger particles. Since bigger particles play a major role in determining the total mass, it can be said that the mass concentration-based removal efficiency increases when large particles are captured. Number concentrations provide a more accurate representation of sub-micron particles. This was the reason why there are differences between number concentration-based removal efficiencies and mass concentration-based removal efficiencies. On this basis, as also verified in Figure 4.5 and Figure 4.6, it can be said that the conductive nanomaterial-decorated nylon mesh filters were more successful at capturing large particles, as many filters on the market do. As shown in Figure 4.7, high mass concentration-based removal efficiency values were achieved due to high removal efficiency of particles larger than 1 μm.

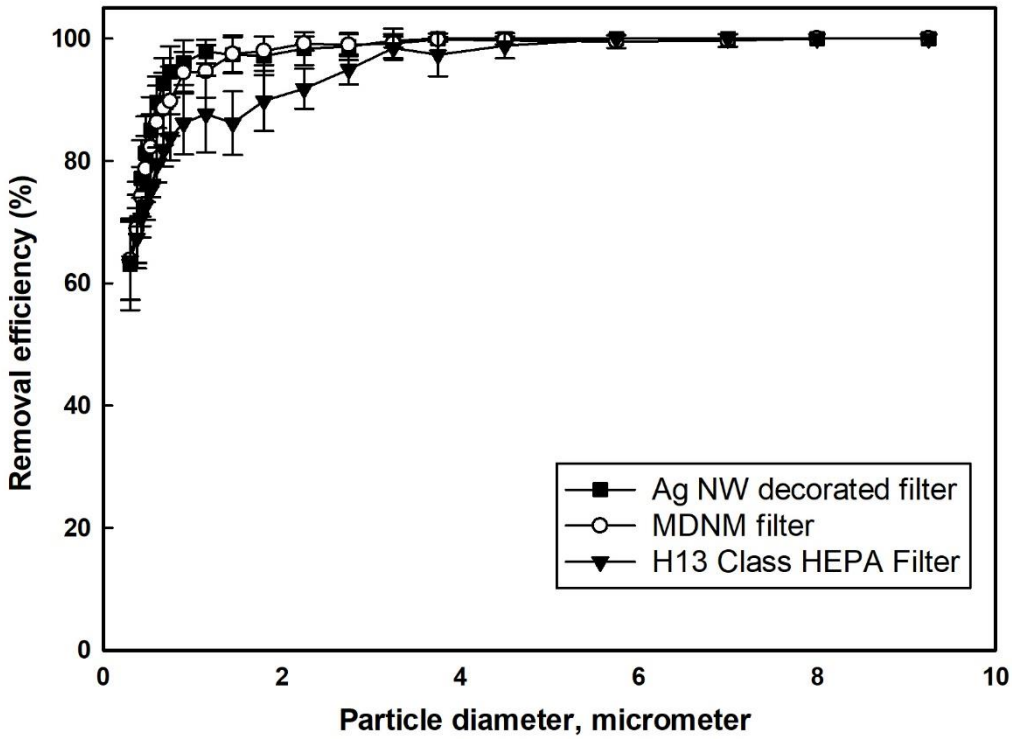

Figure 4.7 Mass concentration-based removal efficiencies of filters according to particle size.

4.3.2 The effect of air velocity on filtration performance of nanomaterial-decorated filters

Air permeability plays an important role in evaluating the performance of an air filter. Pressure drop, which is used to simplify the air permeability, is related to air velocity. The pressure drops of conductive nanomaterial-decorated nylon mesh filters and H13 class HEPA filter were measured with a digital pressure gauge at two different air velocities of 0.45 m/s and 1.02 m/s, are provided in Figure 4.8.

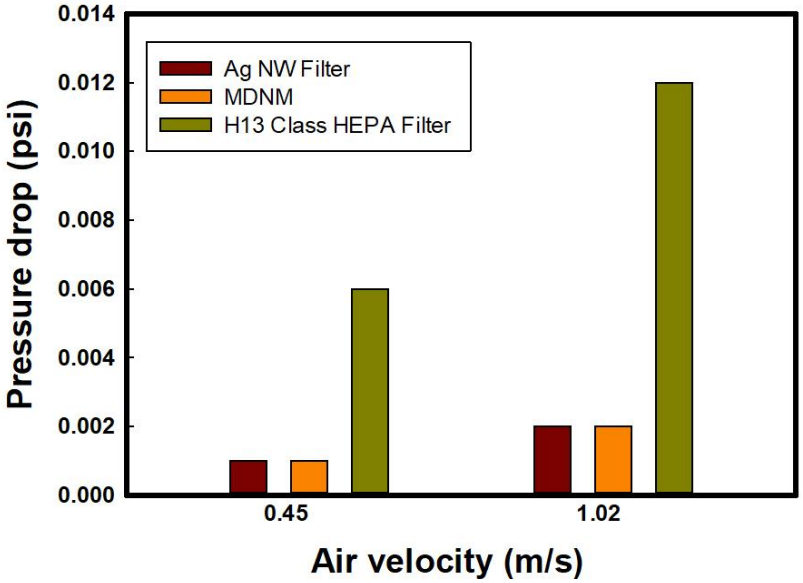

Figure 4.8 Pressure drop of filters according to the air velocity.

As filter is used, it gets clogged and its permeability decreases. This causes an increase in airflow resistance of filter during filtration, and thus increases pressure drop. In order to maintain the same airflow rate as the filter gets clogged, the speed of the fan should be increased in order to compensate the increased airflow resistance of filter. This causes an increase in the energy consumption. In order not to increase this consumption, the development of effective filters with low pressure drop is needed. Under lower air velocity (0.45 m/s), pressure drop was measured as 0.001 psi for MDNM and Ag NW filters while it was 0.006 psi for HEPA filter (Figure 4.8). For higher air velocity (1.02 m/s), pressure drop is measured as 0.002 psi for MDNM filters and Ag NW-decorated filters while it was 0.012 psi for HEPA filter. An extremely low-pressure drop was obtained for conductive nanomaterial-decorated nylon mesh filters. This was, because nylon mesh has large openings compared to commercial HEPA filters. Most of the HEPA filters have a pore sizes of 0.3 μm, which is MPPS. This was the actual reason of using nylon mesh filters in the first place. Secondly, the conductive nanomaterial-decorated onto the surface of the nylon mesh do not increase the diameter of the nylon mesh fibers and therefore do not obstruct air flow.

The average removal efficiencies of conductive nanomaterial-decorated nylon mesh filters and H13 class HEPA filter were calculated for two different air velocities studied, are illustrated in Figure 4.9. The applied voltage for nanomaterial-decorated nylon mesh filters was 10 V. Although lower pressure drops were obtained during lower air velocities, it was observed that the filters capture PM more efficiently at higher air velocity.

According to mass concentration-based removal efficiency calculations, Ag NW decorated filters reached removal efficiencies of 81.65% and 88.32% for $PM_{2.5}$ and PM_{10} at the air velocity of 0.45 m/s, respectively. According to number concentration-based removal efficiency calculations, Ag NW-decorated filters reached removal efficiencies of 66.29% and 66.35% for $PM_{2.5}$ and PM_{10} at the air velocity of 0.45 m/s, respectively. According to mass concentration-based removal efficiency calculations, Ag NW-decorated filters reached removal efficiencies of 90.98% and 96.11% for $PM_{2.5}$ and PM_{10} at the air velocity of 1.02 m/s, respectively. According to number concentration-based removal efficiency calculations, Ag NW-decorated filters reached removal efficiencies of 70.98% and 71.21% for $PM_{2.5}$ and PM_{10} at the air velocity of 1.02 m/s, respectively.

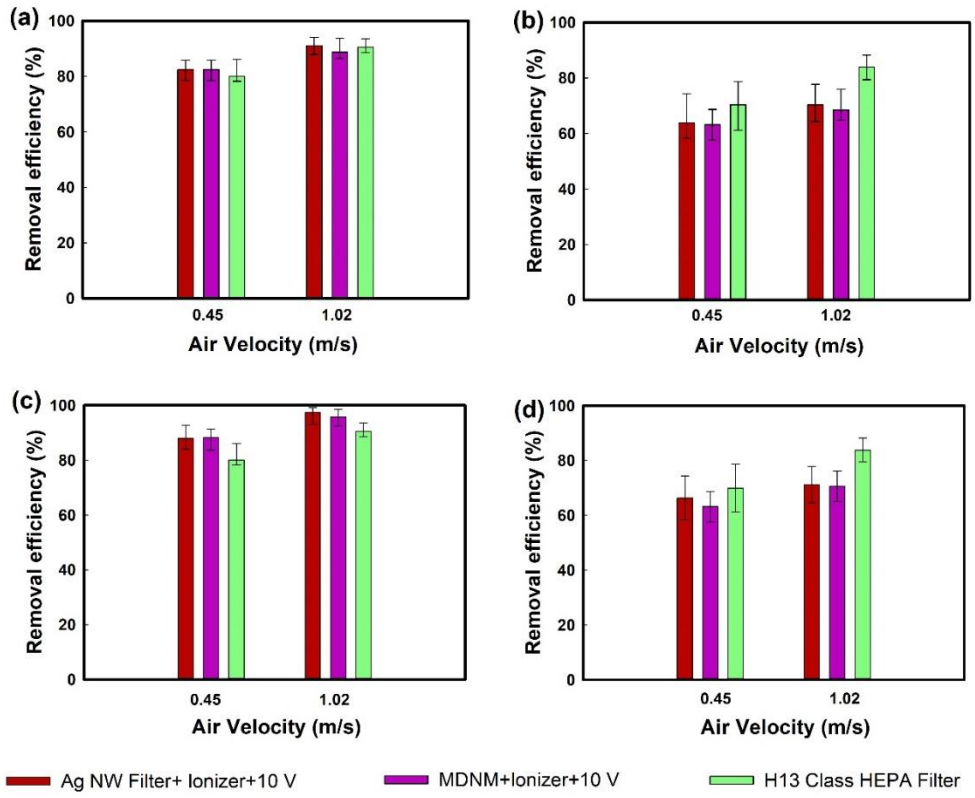

Figure 4.9 $PM_{2.5}$ removal efficiencies of filters based on (a) mass concentration, and (b) number concentration; PM_{10} removal efficiencies of filters based on (c) mass concentration, and (d) number concentration.

Regarding MDNM filter filtration tests, based on mass concentration-based removal efficiency calculations, MDNM filters reached removal efficiencies of 82.14% and 87.51% for $PM_{2.5}$ and PM_{10} at an air velocity of 0.45 m/s, respectively (Figure 4.9). According to number concentration-based removal efficiency calculations, MDNM filters reached removal efficiencies of 63.13% and 63.21% for $PM_{2.5}$ and PM_{10} at an air velocity of 0.45 m/s, respectively. According to mass concentration-based removal efficiency calculations, MDNM filters reached removal efficiencies of 90.05% and 95.44% for $PM_{2.5}$ and PM_{10} under an air velocity of 1.02 m/s, respectively. According to number concentration-based removal efficiency calculations, MDNM filters reached removal efficiencies of 70.37% and 70.58% for $PM_{2.5}$ and PM_{10} at an air velocity of 1.02 m/s, respectively.

Considering the HEPA filter filtration tests, according to mass concentration-based removal efficiency calculations, H13 class HEPA filter reached removal efficiencies of 82.16% and 88.40% for $PM_{2.5}$ and PM_{10} at an air velocity of 0.45 m/s, respectively (Figure 4.9). According to number concentration-based removal efficiency calculations, H13 class HEPA filter reached removal efficiencies of 69.95% and 70.02% for $PM_{2.5}$ and PM_{10} at an air velocity of 0.45 m/s, respectively. According to mass concentration-based removal efficiency calculations, H13 class HEPA filter reached removal efficiencies of 91.03% and 94.51% for $PM_{2.5}$ and PM_{10} at an air velocity of 1.02 m/s, respectively. According to number concentration-based removal efficiency calculations, H13 class HEPA filter reached removal efficiencies of 83.81% and 83.84% for $PM_{2.5}$ and PM_{10} at an air velocity of 1.02 m/s, respectively.

Air flow rate, which is one of the factors that significantly affect the performance of air filters, also affects the contribution of filtration mechanisms. Diffusion and electrostatic force become dominant mechanisms under low air flow rates. Lower air velocity provides longer retention time for airborne particles leading to lower penetration and thus higher removal efficiencies (Huang et al., 2013; Mahdavi, 2013). Under high air flow rate, interception becomes a dominant mechanism. On the other hand, the pattern of flow, which can be affected by air flow rate, is another parameter that can influence the performance of air filters (Tcharkhtchi et al., 2020).

In this study, contrary to the general belief in the literature (Mahdavi, 2013), it was observed that the removal efficiency increases with the air velocity. This result was obtained both in H13 class HEPA filter, which capture PM with the combination of different filtration mechanisms, and in conductive nanomaterial decorated nylon mesh filters, which capture PM mainly via electrostatic attraction force along with the different filtration mechanisms. Therefore, considering the air velocities studied here, it can be said that the results obtained in this study was not mainly dependent on the filtration mechanism that changes depending on the air velocity. These results can be attributed to unsteady pattern of air flow, which is another parameter that can

be less effective in filtration performance (Tcharkhtchi et al., 2020). The low air velocity may have caused an unsteady or insufficient airflow in the filtration set-up.

4.3.3 Assessment of nanomaterial-decorated filters' repeatability, reusability, and 2-hour filtration performance

4.3.3.1 Repeatability of nanomaterial-decorated filter production

Repeatability tests were performed, after determining the optimum voltage value and optimum air velocity for conductive nanomaterial-decorated nylon mesh filters. It is important to produce identical air filters with similar filtration performances in an easily repeatable manner by using the same procedure. In this study, repeatability refers to having similar characteristics before and after filtration, and similar filtration performances. In order to characterize, resistances of three identical filters were measured. These resistances were 52.0 Ω, 51.5 Ω, and 53.4 Ω for Ag NW-decorated filters. For MDNM filters, resistances were measured as 54.1 Ω, 55.0 Ω, and 53.7 Ω.

Three identical filters were subjected to same filtration tests, results of which are shown in Figure 4.10 and Figure 4.11, for Ag NW-decorated filters and MDNM filters, respectively. These results were obtained by repeated filtration tests performed 5 times for each of the three replicates of both filter types.

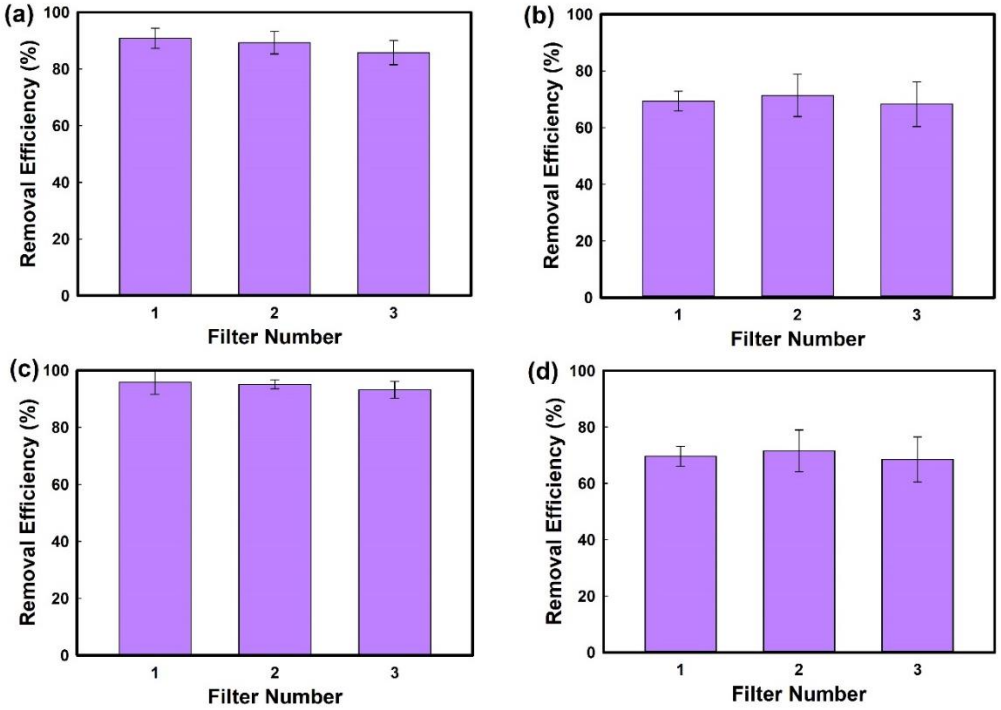

Figure 4.10 $PM_{2.5}$ removal efficiencies of Ag NW-decorated filters based on (a) mass concentration, and (b) number concentration; PM_{10} removal efficiencies of Ag NW-decorated filters based on (c) mass concentration, and (d) number concentration.

According to mass concentration-based removal efficiency calculations, Ag NW-decorated filters reached removal efficiencies of 92.31%, 89.66%, 87.43% and 98.55%, 93.68%, 93.76% for $PM_{2.5}$ and PM_{10}, respectively (Figure 4.10). According to number concentration-based removal efficiency calculations, Ag NW-decorated filters reached removal efficiencies of 68.46%, 73.51%, 65.23% and 69.57%, 73.59%, 65.36% for $PM_{2.5}$ and PM_{10}, respectively (Figure 4.10).

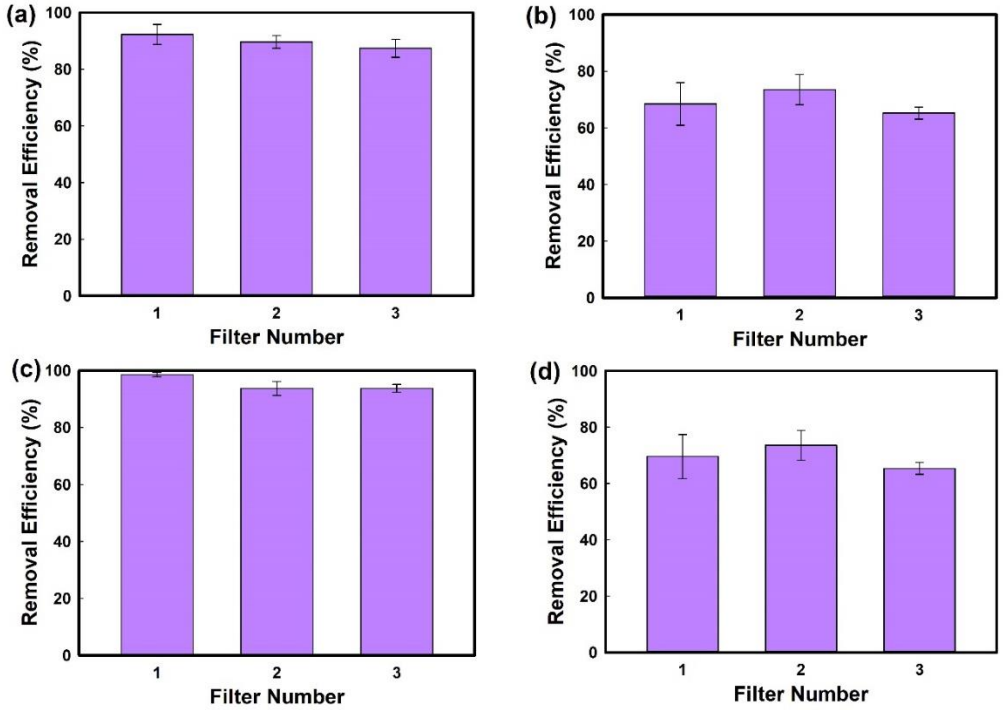

Figure 4.11 $PM_{2.5}$ removal efficiencies of MDNM filters based on (a) mass concentration, and (b) number concentration; (c) PM_{10} removal efficiencies of MDNM filters based on mass concentration, and (d) number concentration.

According to mass concentration-based removal efficiency calculations, MDNM filters reached removal efficiencies of 90.83%, 89.27%, 85.81% and 95.83%, 95.06%, 93.22% for $PM_{2.5}$ and PM_{10}, respectively (Figure 4.11). According to number concentration-based removal efficiency calculations, MDNM filters reached removal efficiencies of 69.36%, 71.39%, 68.31% and 69.63%, 71.53%, 68.48% for $PM_{2.5}$ and PM_{10}, respectively (Figure 4.11).

The removal efficiency can be affected by the changes in indoor air, as shown in Figure 4.3. Especially for smaller particles such as PM_1, it was hard to obtain the same amount of particles for all filtration tests. However, removal efficiencies for identical filters were close to each other throughout the cycles. This demonstrated the repeatability of the conductive nanomaterial-decorated nylon mesh filters

production. As shown in Figure 4.12, filters had also same pressure drop (0.002 psi) during all filtration tests.

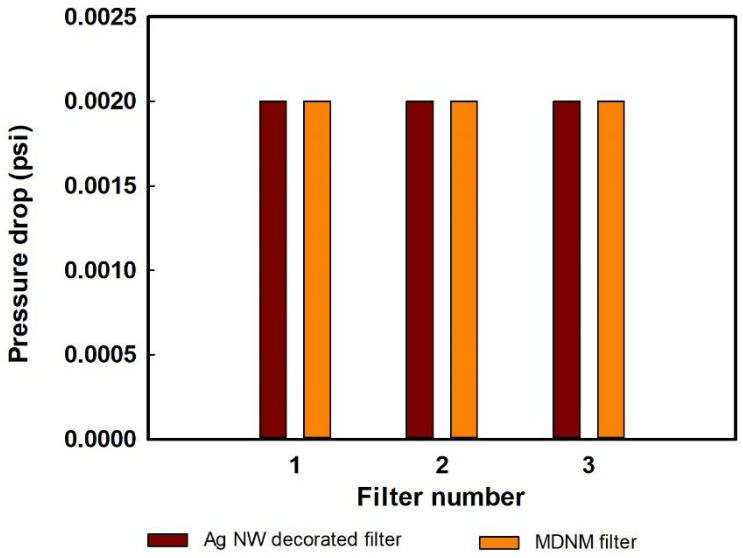

Figure 4.12 Average pressure drop values of developed filters.

4.3.3.2 Reusability of nanomaterial-decorated filters

Since air filters gets clogged in time, they need to be periodically replaced. It is very important to develop reuse procedures to eliminate this need. The reuse of filtration materials provides a cost advantage and decrease filter waste. In this study, airborne particles on the conductive nanomaterial-decorated nylon mesh filters were removed by the polarity of a solvent.

For both conductive nanomaterial-decorated nylon mesh filters, ethylene glycol was preferred as a polar solvent since it is used in many studies due to its high dipole moment (Jeong et al., 2017; Zhang and Hsieh., 2020; Han et al., 2021b). Given in Section 3.4.2.4, washing procedure and filtration tests were repeated five times. The electrical resistance of the filter was measured after each washing process. The PM removal efficiency performance of Ag NW-decorated nylon mesh filters along with filter washing are summarized in Figure 4.13.

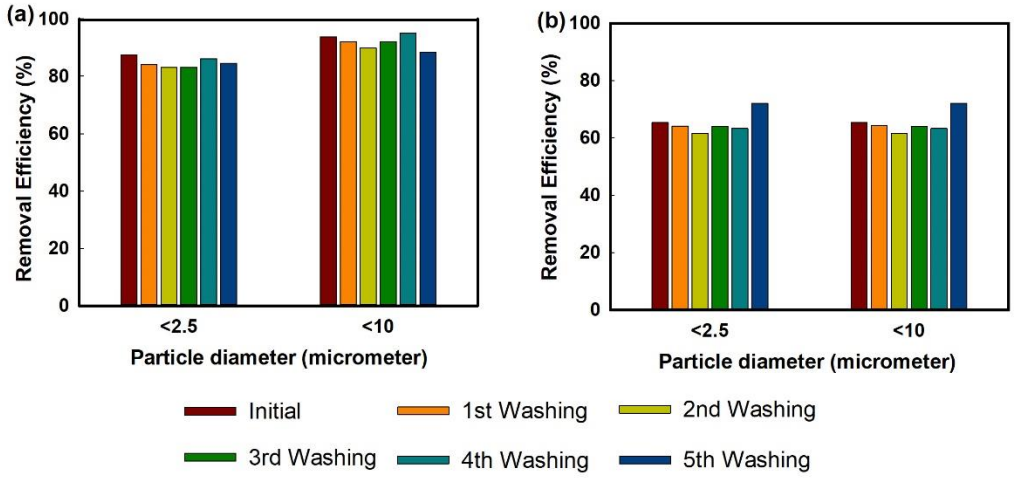

Figure 4.13 PM removal efficiency of polar solvent-washed Ag NW-decorated filters based on (a) mass concentration, and (b) number concentration.

Through strong dipole-dipole interactions between the dipole solvent and the PM, the majority of the particles accumulated on the fibers are successfully removed without causing any harm to the filter. Remarkably, the Ag NW-decorated nylon mesh filter retained its removal performance with superior durability and reliability for repeated usage even after five cycles of the filtration-washing process. As shown in Figure 4.14a, there was no change in pressure drop, it was measured as 0.002 psi in all cycles. On the other hand, the electrical resistance of Ag NW-decorated nylon mesh filter showed a slight change, which was still in the range of 0-1 Ω (Figure 4.14b). Thus, the Ag NW-decorated nylon mesh filter seemed to be reusable even after 5th filtration and washing cycle. This result was comparable to the other similar studies in the literature. Both Jeong et al. (2017) and Narakaew et al. (2022) used same polar solvent, ethylene glycol, to clean their Ag NW-decorated nylon filters. After 5 cycles of filtration-washing process, they maintained their filtration performance.

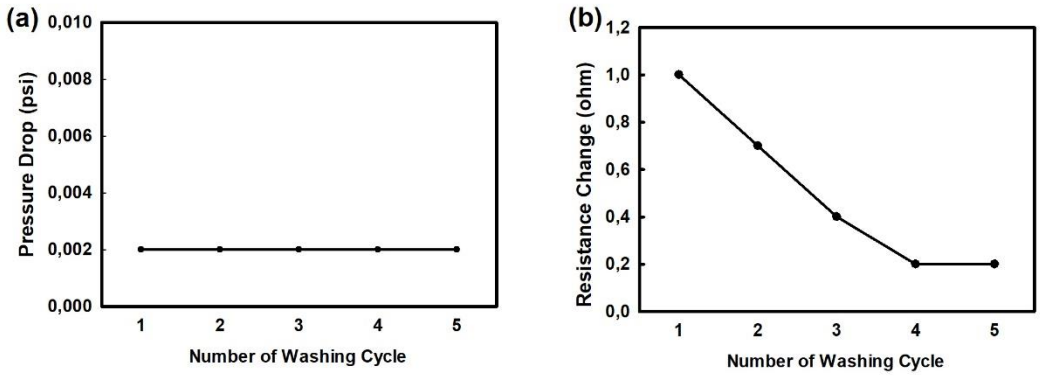

Figure 4.14 (a) Change in pressure drop during filtration with Ag NW-decorated filter after each washing cycle, (b) Electrical resistance change for the Ag NW filter reusability. Lines are for visual aid.

FT-IR spectroscopy was performed within the wavenumber range of 4000 to 400 cm^{-1} in transmission mode, to determine the chemical bond changes of the Ag NW-decorated nylon mesh filters upon cleaning. Confirmed by the corresponding FT-IR spectra, which is given in Figure 4.15, airborne particles were completely removed from the filter by a simple washing process without causing any damage on the Ag NW network. In parallel with the examples in the literature, the unused Ag NW-decorated nylon mesh filter and washed Ag NW-decorated nylon mesh filter had similar signal trends, while the used Ag NW-decorated nylon mesh filter showed different signal trends within 700−1800 cm^{-1} (Jeong et al., 2017; Huang et al., 2019). The peaks from 1700 cm^{-1} to 1000 cm^{-1} can be attributed to the C-O and C=O bondings. As shown in Table 4.3, the biggest composition of PM was elemental carbon. Thus, as it is seen in Figure 4.15, the carbon content of the filter, which increased after filtration, decreased back to its original content similar to the characteristics before its first use. This also reveals that washing removes only PM captured on the Ag NW-decorated nylon mesh filter and does not cause any damage to the filter.

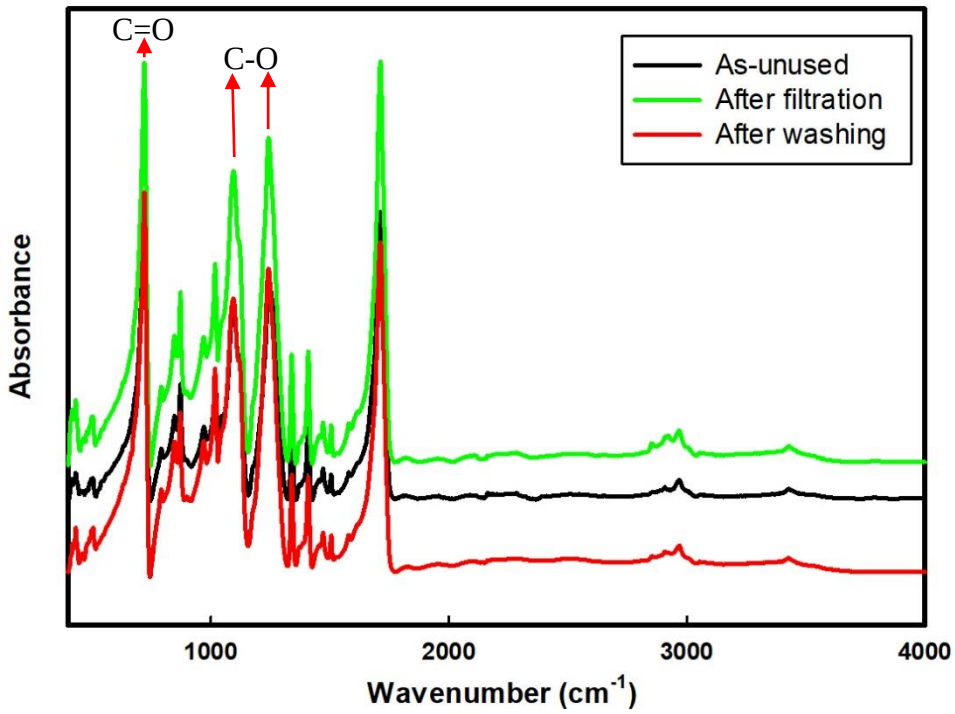

Figure 4.15 FT-IR investigation of Ag NW-decorated nylon mesh filter upon washing.

For MDNM filters, polar solvent washing via ethylene glycol procedure was found to be inappropriate. After only one washing, the electrical resistance of MDNM filter showed a significant increase to 100 Ω. This increase caused the applied voltage not to lead to sufficient current, so the filter lost its function. Therefore, based on Jung et al. (2018), deionized water was chosen as polar solvent. As shown in Figure 4.16a, there was no change in pressure drop and it was measured as 0.002 psi in all cycles. Although there was a resistance change of 10-20 Ω for each washing cycle, there was a significant change in the removal efficiency of the filter after the second wash. Figure 4.16b shows an electrical resistance change for the MDNM filter reusability. Since MXene's conductivity was not as high as Ag NW, even this amount of decrease in conductivity caused the filter to significantly lose the electrostatic power it created to capture PM. The cycle including the filtration test and washing procedure was not repeated 5 times, as the removal efficiency was found to decrease by approximately

10%. The PM removal efficiency of MDNM filters along with filter cleaning are summarized in Figure 4.17.

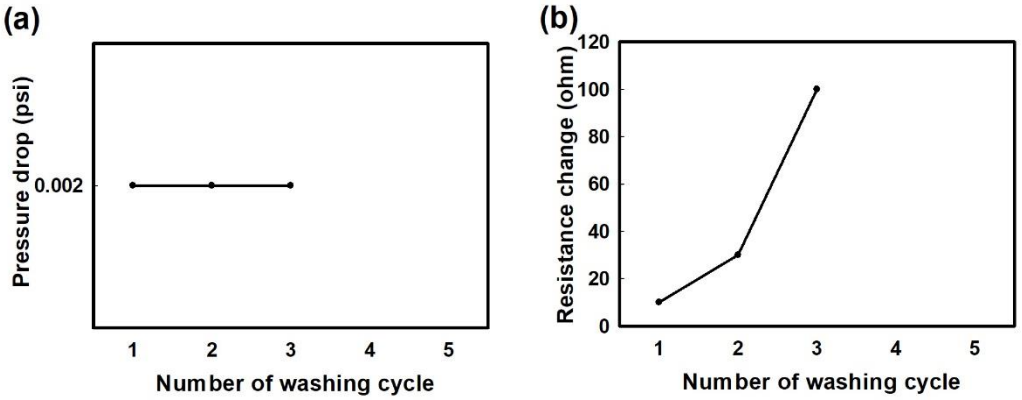

Figure 4.16 (a) Change in pressure drop during filtration with MDNM filter after each washing cycle, (b) Electrical resistance change for the MDNM filter reusability. Lines are for visual aid.

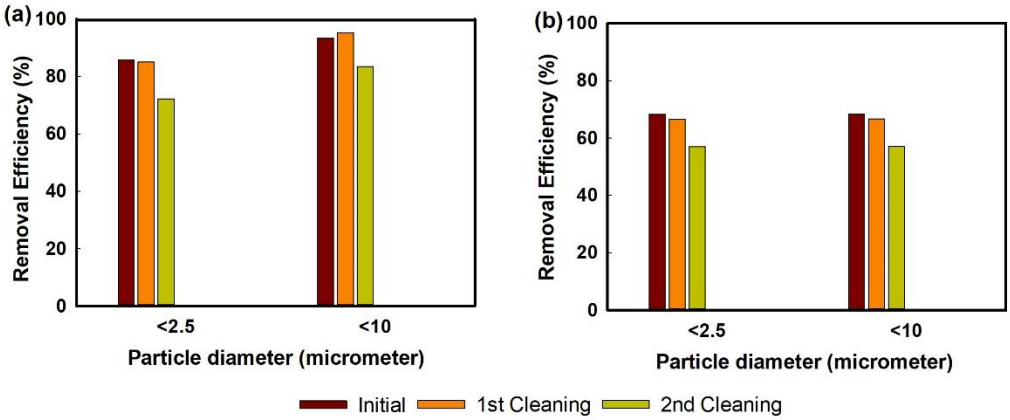

Figure 4.17 PM removal efficiency of polar solvent-washed MDNM filters based on (a) mass concentration, and (b) number concentration.

FT-IR spectroscopy was performed within the wavenumber range of 4000 to 400 cm^{-1} in transmission mode, to determine the changes in chemical bonds of the MDNM filter upon washing. Confirmed by the corresponding FT-IR spectra, which is given in Figure 4.18, deionized water washing process caused damages on the

MXene network on filter surface. Peak trends, weakened at 716 cm^{-1} and 870 cm^{-1}, can be explained by the weakened Ti-O and C-F bonds, respectively. This proves changes in MXene structure due to washing. MXene nanosheets are known to disperse easily in water and several polar organic solvents due to their hydrophilicity, which is enabled by terminal groups such as –OH (Zhao et al., 2020).

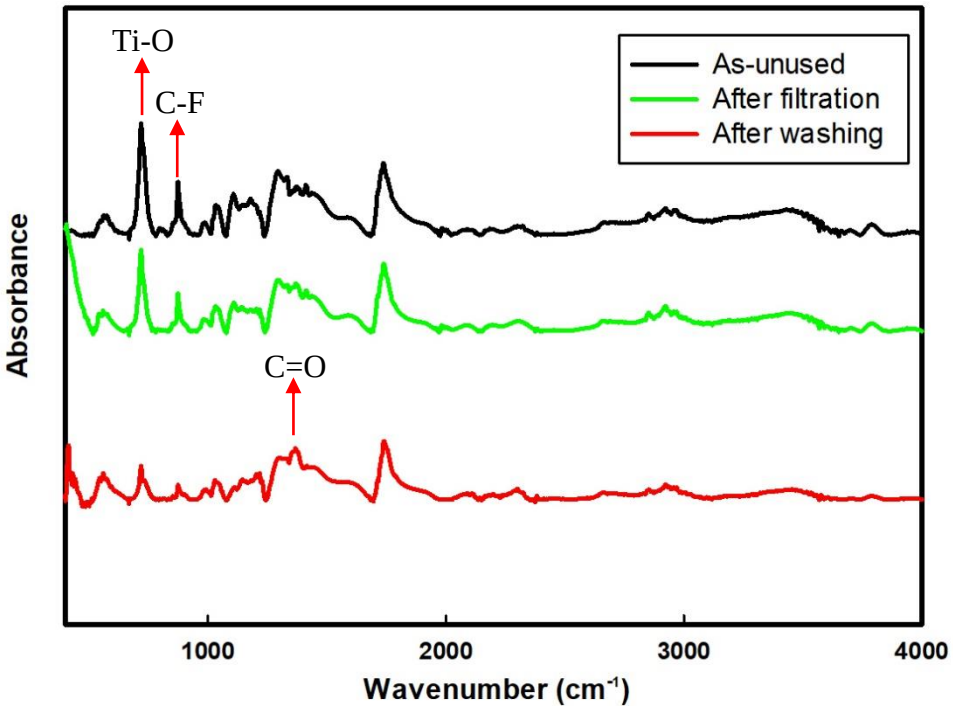

Figure 4.18 FT-IR investigation of MDNM filter.

4.3.3.3 2-hour filtration test performance of nanomaterial-decorated filters

The long-term utilization is very important for the practical application of air filters. One of the main reason is that, it is not easy for consumers to replace the commercially available filters that are extensively utilized in public areas. Also, filters that need to be changed frequently cause an increase in the operational cost. The other main reason is that, long-term exposure to air pollution can lead to a wide range of health problems and environmental effects.

In order to make a prediction for the long-term performances of the conductive nanomaterial-decorated nylon mesh filters, the developed filters were tested for 2 hours at 10 V and 1.02 m/s. The filtration tests were repeated 5 times for both filter types, Ag NW-decorated filters and MDNM filters; that is, each filter type was operated for a total of 20 hours. Pressure drop measurements at the end of each hour were given in Figure 4.19. The 2-hour filtration removal efficiencies of Ag NW-decorated filters and MDNM filters are shown in Figure 4.20 and Figure 4.21, respectively.

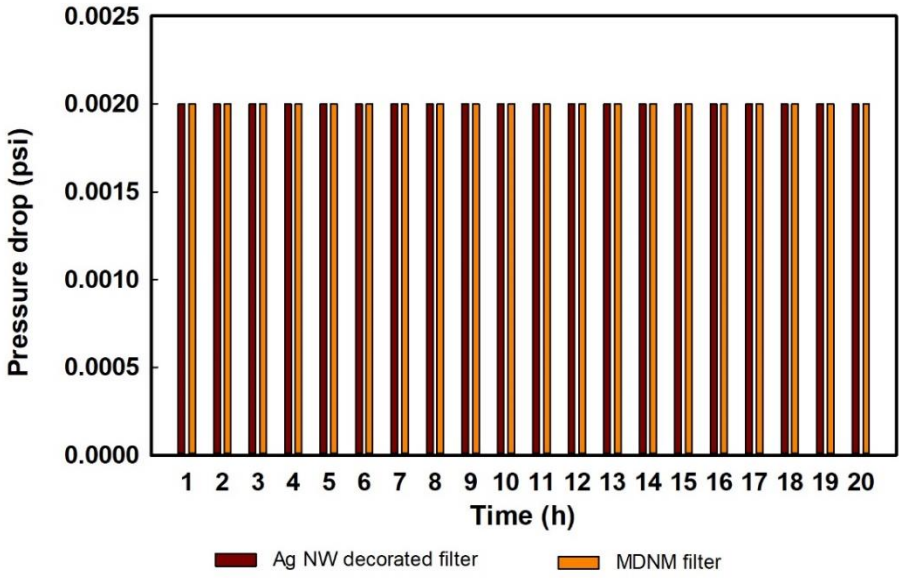

Figure 4.19 Average pressure drop values of developed filters for 2 hours.

According to mass concentration-based removal efficiency calculations, Ag NW-decorated filters had removal efficiency ranges of 85.71-96.53% and 90.02-98.21% for $PM_{2.5}$ and PM_{10} for 2 hours, respectively. According to number concentration - based removal efficiency calculations, Ag NW-decorated filters had removal efficiency ranges of 78.20-88.80 % and 78.23-88.94% for $PM_{2.5}$ and PM_{10} for 2 hours, respectively.

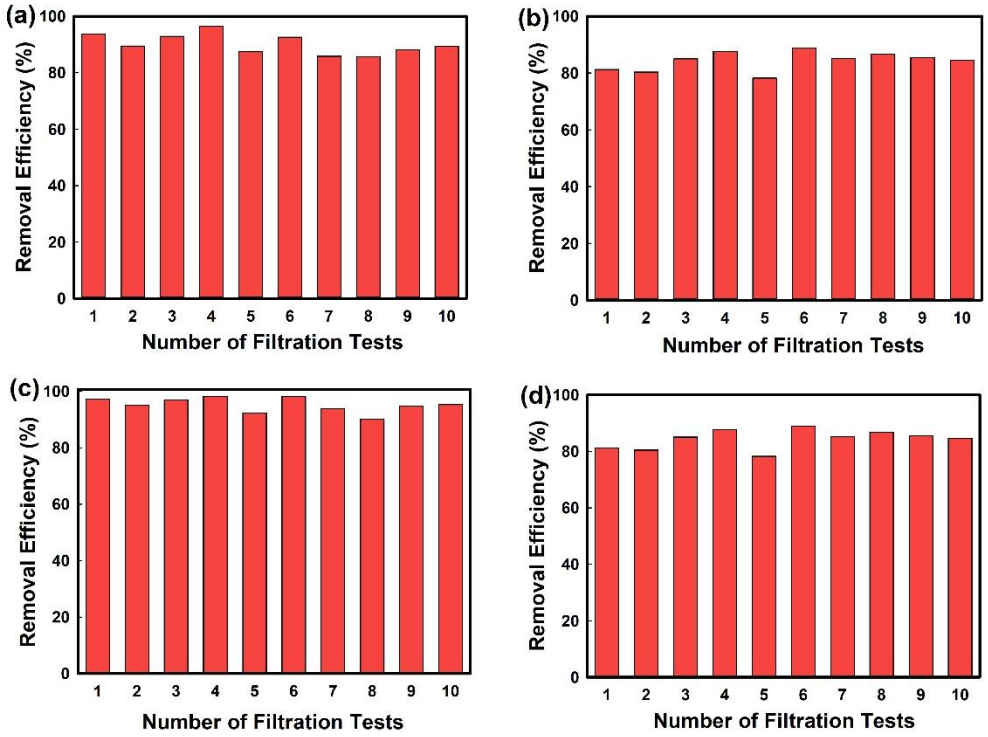

Figure 4.20 2-hour $PM_{2.5}$ removal efficiencies of Ag NW-decorated filters based on (a) mass concentration, and (b) number concentration; 2-hour PM_{10} removal efficiencies of Ag NW-decorated filters based on (a) mass concentration, and (d) number concentration.

According to mass concentration-based removal efficiency calculations, MDNM filters had removal efficiency ranges of 84.13-94.41% and 87.57-97.07% for $PM_{2.5}$ and PM_{10} for 2 hours, respectively. According to number concentration -based removal efficiency calculations, MDNM filters had removal efficiency ranges of 67.93-86.84% and 67.96-86.90% for $PM_{2.5}$ and PM_{10} for 2 hours, respectively.

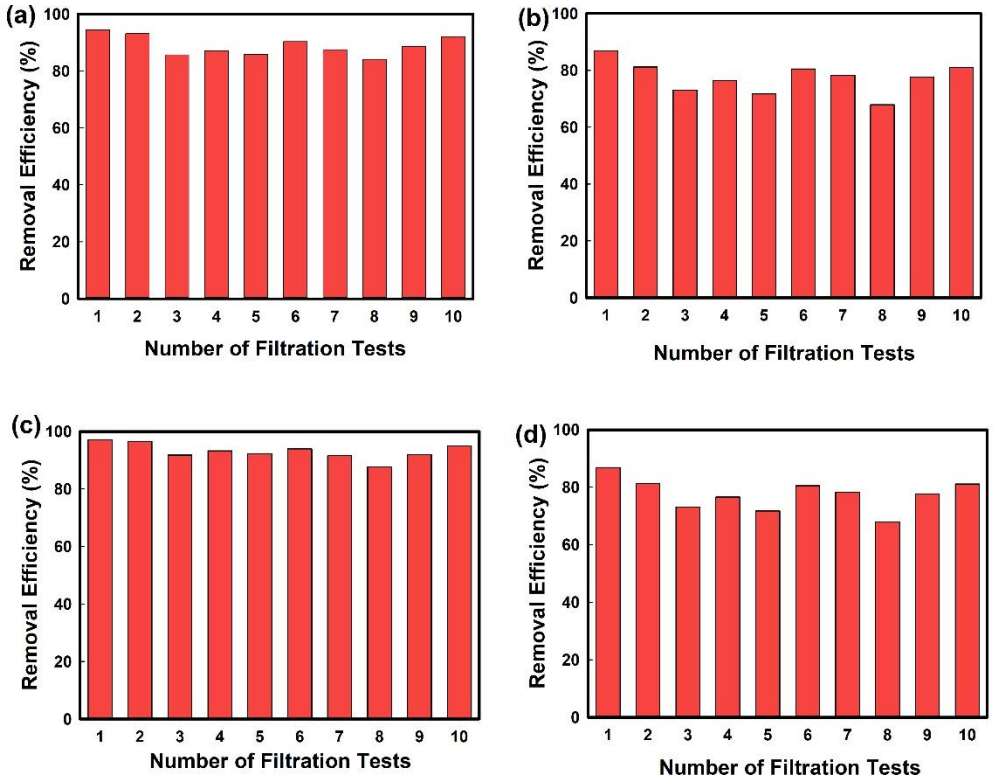

Figure 4.21 2-hour $PM_{2.5}$ removal efficiencies of MDNM filters based on (a) mass concentration, and (b) number concentration; (c) 2-hour PM_{10} removal efficiencies of MDNM filters based on (c) mass concentration, and (d) number concentration.

Nanomaterial-decorated nylon mesh filters maintained their removal efficiencies for 2 hours. Besides, considering the results of previous studies (Figure 4.5, Figure 4.6, Figure 4.9, Figure 4.10, Figure 4.11, Figure 4.13, and Figure 4.17), the difference between mass concentration-based removal efficiencies and number concentration-based removal efficiencies decreased. Thanks to the increased filtration time, the filters had also reduced the number of particles. As the residence time increased, the probability of collision between the particle and the filter increased considerably (Mahdavi, 2013). In addition, the fact that there was no change in pressure drop even after 2 hours indicates that the permeability of filters was not decreasing (Figure 4.19). Low pressure drop implies that there was not an increase in airflow resistance of filter. Therefore, there is no need for powerful, energy-intensive, and expensive pumps to generate sufficient airflow against high pressure drop across the filter. As

a result, there was no need for more energy consumption and more operating cost. Fabricated filters can be used for a long time without changing.

CHAPTER 5

CONCLUSIONS AND FUTURE WORK

In this thesis, nylon mesh coated with two different conductive nanomaterials (Ag NW and MXene) were developed to improve indoor air quality by PM filtration. It was found that Ag NW and titanium-based MXenes are promising nanomaterials for air filtration due to their excellent properties such as high specific surface area.

Filtration performance of developed filters was evaluated by removal efficiency and pressure drop. A commercial HEPA filter, which is in the filter class of H13, was also tested as a reference filter. The significant observations and results were listed as follows:

- In order to investigate the effect of voltage application, different voltages (2.5 V, 5 V, 7.5 V, or 10 V for Ag NW-decorated filters; 5 V and 10 V for MDNM filters) were studied. Since the nylon mesh was heated up through voltage application, maximum voltage of 10 V was applied to the filters.

    - For both nanomaterial-decorated filter types, the best PM removal performance was obtained when the ionizer was on and the applied voltage on the decorated filter was adjusted to 10 V. Results demonstrated that the removal efficiency was enhanced with the electrical conductivity of nanomaterial networks. Because of this conductivity, a strong interaction occurred between positively-charged nylon mesh filters and negatively-charged particles.

- For $PM_{2.5}$, mass concentration-based removal efficiencies were 90.98% and 90.05% for Ag NW-decorated filters and MDNM filters, respectively. For PM_{10}, the results of mass concentration-based removal efficiencies were 96.11% and 95.44% for Ag NW-decorated filters and MDNM filters, respectively.

- For $PM_{2.5}$, the results of number concentration-based removal efficiencies were 70.98% and 71.21% for Ag NW-decorated filters and MDNM filters, respectively. For PM_{10}, the results of number concentration-based removal efficiencies were 70.37% and 70.58% for Ag NW-decorated filters and MDNM filters, respectively.

- The removal efficiency of the HEPA filter used was lower than the technical specifications datasheet of HEPA filter (99.95%). Mass concentration-based calculations showed that HEPA filter had a removal efficiency of 91.03% for $PM_{2.5}$. This difference can be due to the use of a single particle counter while performing the filtration tests in the fabricated measurement set-up.

- The results of the filtration tests, regarding the mass concentration-based removal efficiency calculation values, revealed that the conductive nanomaterial-decorated nylon mesh filters and HEPA filter under the studied conditions and used filtration set-up, were similar to each other.

- Nylon mesh is a cheap and easily accessible material. After being decorated with conductive nanomaterials, it achieved HEPA quality mass concentration based-removal efficiencies even in single-layer use. In addition, the developed filters have avoided excessive energy consumption, thanks to their much lower pressure drops than HEPA. Yet, there is still potential for improvement in terms of number concentration-based removal efficiency

performance despite the low pressure drops and the promising mass concentration-based removal efficiencies.

- The removal efficiencies were calculated according for both mass concentration and number concentration. The mass concentrations of particles are computed based on the assumptions that all particles have a spherical shape and a uniform density.

    - Since bigger particles play a major role in determining the total mass, it can be said that the mass-based removal efficiency increases when large particles are captured. This could be the cause of the difference in removal efficiencies between two approaches. On the basis of this, it can be said that nylon mesh filters decorated with conductive nanomaterials are more effective at capturing big particles as many other filters on the market.

- In this thesis, the effect of air velocity on filtration performance was also investigated at two different air velocities, namely, 0.45 m/s and 1.02 m/s.

    - Due to the large openings of nylon mesh, a low-pressure drop was obtained for developed filters. Also, nanomaterial decoration did not increase the diameter of the nylon mesh fibers and therefore did not increase the resistance to air flow. Therefore, the developed filters do not require powerful pumps like most of HEPA filters do.

    - All filters used in this study capture PM more efficiently at higher air velocities. These results can be related with the unsteady pattern of airflow or the insufficient airflow in the filtration set-up at lower air velocity studied.

- Removal efficiencies and pressure drops of three identical filters remained consistent with each other. This was a proof demonstrating that conductive nanomaterial nylon mesh filters can be produced in a repeatable manner.

- The reusability of the filters was tested, as it is more cost-effective and environmentally advantageous to reuse the filters than to replace them or buy new ones.

    - Ag NW-decorated nylon mesh filter retained its removal efficiency and low pressure drop values for repeated usage even after five cycles of the filtration-cleaning process. Polar solvent washing via ethylene or deionized water was found to be not appropriate for MDNM filters.

- Long-term use of air filters is very important in terms of cost, operational convenience, and reduction of long-term exposure to air pollution. Nanomaterial-decorated nylon mesh filters maintained their removal efficiencies and low pressure drop for 2 hours under the optimum conditions determined (applied voltage of 10 V and airflow velocity of 1.02 m/s). These results are the starting point of long-term experiments, which remains to be investigated.

Recommendations for future work based on the findings in this study are given as follows:

- Most of the studies in literature were conducted on laboratory scale measurement set-ups. Different sizes of filters can be produced and their use in field scale can be investigated.

- The application area of the developed filters can be extended, by using filters in passive air purification solutions such as curtains. In this way, the energy consumption could be decreased further.

- A detailed cost analysis can be done to compare the nanomaterial-decorated nylon mesh filters with conventional air filters.

- Nylon mesh filters with smaller pore sizes can be investigated for coating with the Ag NW and MXene in order to enhance the removal efficiency of smaller particles such as PM_1.

- Since the used nanomaterials can be easily decorated onto many materials with different openings, the use of nanomaterials can be improved by decorating them onto different materials such as recycled textiles. From an environmental point of view, developed filters might be beneficial not only for air pollution control but also for waste management.

- The effect of the air velocity on the filtration performance can be investigated in more depth for higher velocities.

- According to current studies and as also confirmed in this thesis, increasing the voltage significantly improves PM removal effectiveness. Therefore, the

voltage application can be extended by choosing materials that can withstand the high heatings caused by high voltages.

- Different reuse procedures can be explored to increase the stability of MXene.

- It is known that nanosilver and MXene have antibacterial activity. Although there are studies conducted on this subject, the studies on removal efficiency of bacteria in air are limited and remains to be investigated.

REFERENCES

Aramendia, I., Fernandez-Gamiz, U., Lopez-Arraiza, A., Rey-Santano, C., Mielgo, V., Basterretxea, F. J., Sancho, J., & Gomez-Solaetxe, M. A. (2018). Experimental and Numerical Modeling of Aerosol Delivery for Preterm Infants. *International journal of environmental research and public health*, *15*(3), 423. https://doi.org/10.3390/ijerph15030423

Atwa, Y., Maheshwari, N., Goldthorpe, I. A. (2015). "Silver nanowire coated threads for electrically conductive textiles", Journal of Materials Chemistry C, 3(16), 3908–3912. https://doi.org/10.1039/c5tc00380f

Bahçelioğlu, E. (2019). Silver Nanowire Decorated Glass Fiber Filters For Bacteria Removal From Water. Yüksek Lisans Tezi, Orta Doğu Teknik Üniversitesi.

Bahçelioğlu, E., Doganay, Doğa., Coskun, S., Unalan, H. E., Erguder, T. H. (2020). A Point-of-Use (POU) Water Disinfection: Silver Nanowire Decorated Glass Fiber Filters. *Journal of Water Process Engineering*. 38. 10.1016/j.jwpe.2020.101616.

Barhate, R.S., Ramakrishna, S. (2007). Nanofibrous filtering media: filtration problems and solutions from tiny materials. *Journal of Membrane Science* 296, 1-8.

Bingbing, S., Lars, E. E., Sarka, L. (2013). Intermediate Air Filters for General Ventilation Applications: An Experimental Evaluation of Various Filtration Efficiency Expressions. *Aerosol Science and Technology*, 47:5, 488-498, DOI: 10.1080/02786826.2013.766667

Büyüknalçacı, F. N. (2018). Optimization of Solution Blown PVDF Nanofibers for Air Filtration Applications, İstanbul Technical University.

Carruthers, D., Carslaw, D., Colvile, R., Richard Derwent OBE, P., Dorling, S., Bernard Fisher, P., … Stevenson, K. (2005). *Particulate Matter in the United Kingdom*. Retrieved from https://uk-air.defra.gov.uk/assets/documents/reports/aqeg/pm-summary.pdf

Cheng, Y.H. and Lin, Y.L. (2010). Measurement of Particle Mass Concentrations and Size Distributions in an Underground Station. *Aerosol Air Qual. Res.* 10: 22-29. https://doi.org/10.4209/aaqr.2009.05.0037

Cooper, E., Wang, Y., Stamp, S., Burman, E., Mumovic, D. (2021). Use of portable air purifiers in homes: operating behaviour, effect on indoor $PM_{2.5}$ and perceived indoor air quality. *Build. Environ.*, 191, p. 107621, https://doi.org/10.1016/j.buildenv.2021.107621

Coşkun, S., Aksoy, B., Ünalan, H. E. (2011). Polyol synthesis of silver nanowires: An extensive parametric study, *Crystal Growth and Design*, 11(11), 4963–4969. https://doi.org/10.1021/cg200874g

D'Amato, G., Holgate, S. T., Pawankar, R., Ledford, D. K.,… Annesi-Maesano, I. (2015). Meteorological conditions, climate change, new emerging factors, and asthma and related allergic disorders. A statement of the World Allergy Organization. The World Allergy Organization journal, 8(1), 25. https://doi.org/10.1186/s40413-015-0073-0

Ding, L., Wei, Y., Wang, Y., Chen, H., Caro, J., Wang, H. A. (2018). Two-Dimensional Lamellar Membrane: MXene Nanosheet Stacks. *Angew. Chemie*, 129 (7), 1851–1855. https://doi.org/10.1002/ange.201609306

Doğanay, D., Kanicioglu, A., Coskun, S., Akca, G., Ünalan, H. E. (2019). Silver-nanowire-modified fabrics for wide-spectrum antimicrobial applications. *Journal of Materials Research, 34*(04), 500–509. https://doi.org/10.1557/jmr.2018.467

Dong, J., Abukhdeir, N., Goldthorpe, I. (2015). Simple assembly of long nanowires through substrate stretching. *Nanotechnology*. 26. 485302. 10.1088/0957-4484/26/48/485302.

Dorjsuren, U. (2012). İstanbul Üniversitesi Avcılar Yerleşkesi'nde Solunabilir Partikül Maddenin Boyut Dağılımının ve Element İçeriğinin İncelenmesi, Yüksek Lisans Tezi, İstanbul Üniversitesi.
Dökmen, B. (2011). Yüksek Verimli Hava Filtrelerinin Testleri, Yüksek Lisans Tezi, Yıldız Teknik Üniversitesi.

Eom, J., Heo, J.S., Kim, M., Lee, J., Park, S., Kim, YH. (2017). Highly sensitive textile-based strain sensors using poly(3,4-ethylenedioxythiophene):polystyrene sulfonate/silver nanowire-coated nylon threads with poly-L-lysine surface modification. *RSC Advances*. 7. 53373-53378. 10.1039/C7RA10722F.

Esteves, S.C., Varghese, A.C., & Worrilow, K.C. (Eds.). (2016). Clean Room Technology in ART Clinics: A Practical Guide (1st ed.).Chapter 2: Clean room technology: An overview of clean room classification standards CRC Press. https://doi.org/10.1201/9781315372464

Fang, Y., Naik, V., Horowitz, L.W., Mauzerall, D. L. (2013). Air pollution and associated human mortality: the role of air pollutant emissions, climate change and methane concentration increases from the preindustrial period to present. *Atmos Chem Phys*. 13(3): 1377–94. https://doi.org/10.5194/acp-13-1377-2013

Fu, D., Yang, R., Wang, Y., Wang, R., Hua, F. (2022). Silver Nanowire Synthesis and Applications in Composites: Progress and Prospects. *Adv. Mater. Technol.* 2200027. https://doi.org/10.1002/admt.202200027

Fuzzi, S., Baltensperger, U., Carslaw, K., Decesari, S., Denier Van Der Gon, H., Facchini, M. C., … Gilardoni, S. (2015). Particulate matter, air quality and climate: lessons learned and future needs. *Atmospheric Chemistry and Physics*, *15*, 8217–8299. https://doi.org/10.5194/acp-15-8217-2015

Gao, X., Li, Z.-K., Xue, J., Qian, Y., Zhang, L.-Z., Caro, J., Wang, H. Titanium Carbide Ti3C2Tx (MXene) Enhanced PAN Nanofiber Membrane for Air Purification. (2019). *J. Memb. Sci.*, 586, 162–169. https://doi.org/10.1016/j.memsci.2019.05.058

Grimm Aerosol Technik. (2019). MODEL EDM107. Retrieved December 19, 2019, from https://www.grimm-aerosol.com/products-en/environmental-dust-monitoring/approved-pm-monitor/edm107/

Grinshpun, S. A., Mainelis, G., Trunov, M., Adhikari, A., Reponen, T., Willeke, K. (2005). Evaluation of ionic air purifiers for reducing aerosol exposure in confined indoor spaces. *Indoor air*, 15(4), 235–245. https://doi.org/10.1111/j.1600-0668.2005.00364

Guo, M., Zhou, M., Wei, S., Peng, J., Wang, Q., Wang, L., Cheng, D., Yu, W. (2021). Particle removal effectiveness of portable air purifiers in aged-care centers and the impact on the health of older people, *Energy and Buildings,*Volume 250,111250, ISSN 0378-7788, https://doi.org/10.1016/j.enbuild.2021.111250

Gysels, K., Deutsch, F., Grieken, R.V. (2002). Characterisation of particulate matter in the Royal Museum of Fine Arts, Antwerp, Belgium. Atmospheric Environment 36, 4103-4113.

Han, S., Kim, J., Ko, S. H. (2021a). Advances in air filtration technologies: structure-based and interaction-based approaches, *Materials Today Advances,* Volume 9, 100134, ISSN 2590-0498, https://doi.org/10.1016/j.mtadv.2021.100134

Han, S., Kim, J., Lee, Y., Bang, J., Kim, C., Choi, J., Min, J., Ha, I., Yoon, Y., Yun, CH., Cruz, M., Wiley, B., Ko, SH. (2021b). Transparent Air Filters with Active Thermal Sterilization. *Nano Letters*. 22. 10.1021/acs.nanolett.1c02737.

Harrod, K.S., Jaramillo, R.J., Rosenberger, C.L., Wang, S., Berger, J.A., McDonald, J.D. & Reed, M.D. (2003). Increased Susceptibility to RSV Infection by Exposure to Inhaled Diesel Engine Emissions. *American Journal of Respiratory Cell and Molecular Biology*, 28(4):451-63. DOI: 10.1165/rcmb.2002-0100OC

Hemmati, S., Harris, M.T., & Barkey, D.P. (2020). Polyol Silver Nanowire Synthesis and the Outlook for a Green Process. *Journal of Nanomaterials, 2020*, 1-25. DOI:10.1155/2020/9341983

Huang, S-H., Chen, C-W., Kuo, Y., Lai, C.Y., Mckay, R., Chen, C-C. (2013). Factors Affecting Filter Penetration and Quality Factor of Particulate Respirators. *Aerosol and Air Quality Research*. 13. 162-171.

Huang, W. R., He, Z., Wang, J. L., Liu, J. W., Yu, S. H. (2019). Mass Production of Nanowire-Nylon Flexible Transparent Smart Windows for PM2.5 Capture, *iScience*, 12, 333–341. https://doi.org/10.1016/j.isci.2019.01.014

Huczko, A. Template-based synthesis of nanomaterials. *Appl Phys A* 70, 365–376 (2000). https://doi.org/10.1007/s003390051050

Iqbal, A., & Hamdan, N. M. (2021). Investigation and Optimization of Mxene Functionalized Mesoporous Titania Films as Efficient Photoelectrodes. *Materials (Basel, Switzerland)*, *14*(21), 6292. https://doi.org/10.3390/ma14216292

Jeong, S., Cho, H., Han, S., Won, P., Lee, H., Hong, S., Yeo, J.,Kwon, J., Ko, S. H. (2017). High Efficiency, Transparent, Reusable, and Active PM2.5 Filters by Hierarchical Ag Nanowire Percolation Network, *Nano Letters*, 17(7), 4339–4346. https://doi.org/10.1021/acs.nanolett.7b01404

Jung, W., Lee, J. S., Han, S., Ko, S. H., Kim, T., Kim, Y. H. (2018). An Efficient Reduced Graphene-Oxide Filter for $PM_{2.5}$ Removal. *J. Mater. Chem. A*, *6* (35), 16975–16982. https://doi.org/10.1039/C8TA04587A

Kahramantekin, T.A. (2006). Atmosferik partiküllerde iyon analizi ve istatistiksel değerlendirme, Yüksek Lisans Tezi, Anadolu Üniversitesi Fen Bilimleri Enstitüsü.

Kankaria, A., Nongkynrih, B., Gupta, S. (2014). Indoor Air Pollution in India: Implications on Health and its Control. *Indian journal of community medicine: official publication of Indian Association of Preventive & Social Medicine*. 39. 203-7. 10.4103/0970-0218.143019.

Karakaş, B. (2015). İç ve Dış Hava Ortamlarında Partiküler Madde (PM10, PM2.5 ve PM1) Konsantrasyonlarının Değerlendirilmesi. Hacettepe Üniversitesi.

Karaman, B. (2020). Contribution of Mxene Coatings to the Performance of Nickel Based Electroactive Materials, İstanbul Technical University.

Khodashenas, B., & Ghorbani, H. R. (2015). Synthesis of silver nanoparticles with different shapes. *Arabian Journal of Chemistry*. https://doi.org/10.1016/j.arabjc.2014.12.014

Ko, Y. S., , Joe, Y. H., , Seo, M., , Lim, K., , Hwang, J., , & Woo, K., (2014). Prompt and synergistic antibacterial activity of silver nanoparticle-decorated silica hybrid particles on air filtration. *Journal of materials chemistry. B, 2*(39), 6714–6722. https://doi.org/10.1039/c4tb01068j

Koçak, M. (2006). Comprehensive chemical characterization of aerosols in the eastern mediterranean: sources and long range transport, Doktora Tezi, M.E.T.U., The Instıtute Of Marine Sciences, Ankara, 180812.

Kumar, A., Shaikh, M.O., Chuang, C.H. (2021). Silver Nanowire Synthesis and Strategies for Fabricating Transparent Conducting Electrodes. *Nanomaterials*, 11, 693. https://doi.org/10.3390/nano11030693

Kwon, J., Suh, Y. D., Lee, J., Lee, P., Han, S., Hong, S., Yeo, J., Lee, H. Ko, S. H. (2018). Recent progress in silver nanowire based flexible/wearable optoelectronics. *Journal of Materials Chemistry* C, 6(28), 7445–7461. doi:10.1039/c8tc01024b

Lei, J. C., Zhang, X., Zhou, Z. (2015). Recent advances in MXene: Preparation, properties, and applications. *Front. Phys.* 10**,** 276–286. https://doi.org/10.1007/s11467-015-0493-x

Lian, Y., Yu, H., Wang, M., Yang, X., Li, Z., Yang, F., Wang, Y., Tai, H., Liao, Y., Wu, J., Wang, X., Jiang, Y., Tao, G. (2020). A multifunctional wearable E-textile via integrated nanowire-coated fabrics. *Journal of Materials Chemistry C*. 8. 10.1039/D0TC00372G.

Lin, Y., Zou, J., Yang, W., & Li, C. Q. (2018). A Review of Recent Advances in Research on $PM_{2.5}$ in China. *International journal of environmental research and public health*, *15*(3), 438. https://doi.org/10.3390/ijerph15030438

Liu, H., Cao, C., Huang, J., Chen, Z., Chen, G., & Lai, Y. (2020). Progress on particulate matter filtration technology: Basic concepts, advanced materials, and performances. *Nanoscale*, 12(2), 437–453. https://doi.org/10.1039/c9nr08851b

Lv, J., & Zhu, L. (2013). Effect of central ventilation and air conditioner system on the concentration and health risk from airborne polycyclic aromatic hydrocarbons, *Journal of Environmental Sciences*, 25(3), 531–536. https://doi.org/10.1016/S1001-0742(12)60079-5

Mahdavi, A. (2013). Efficiency Measurement of N95 Filtering Facepiece Respirators against Ultrafine Particles under Cyclic and Constant Flows. Masters thesis, Concordia University.

Maroto, M.D. (2011). Filtration Efficiency of Intermediate Ventilation Air Filters on Ultrafine and Submicron Particles. Masters thesis, Chalmers University of Technology.

Müezzinoglu, A. (2005). Hava kirliliği ve kontrolü esasları, Dokuz Eylül Yayınları, İzmir.

Narakaew, S., Thungprasert, S., Janprommin, S., Chaisena, A. (2022). Silver-nanowire/bamboo-charcoal composite percolation network on nylon sheet for improved $PM_{2.5}$ capture efficiency, *Applied Surface Science*, Volume 596,153666, ISSN 0169-4332, https://doi.org/10.1016/j.apsusc.2022.153666

Narcı, E. (2017). Klima Filtre Tozu Örneklerinde Kalıcı Organik Kirleticilerin Seviyelerinin ve Maruziyetlerinin Değerlendirilmesi. Kocaeli Üniversitesi.

National Research Council. (2010). *Global Sources of Local Pollution*. https://doi.org/10.17226/12743

Pandey, R.P., Rasool, K., Madhavan, V.E., Aïssa, B., Gogotsi, Y., & Mahmoud, K.A. (2018). Ultrahigh-flux and fouling-resistant membranes based on layered silver/MXene (Ti3C2Tx) nanosheets. *Journal of Materials Chemistry, 6*, 3522-3533.

Park, K., Kang, S., Park, J-W., Hwang, J. (2021). Fabrication of silver nanowire coated fibrous air filter medium via a two-step process of electrospinning and electrospray for anti-bioaerosol treatment. *Journal of Hazardous Materials*. 411. 125043. 10.1016/j.jhazmat.2021.125043.

Polichetti G., Cocco S., Spinalli A., Trimarco V., Nunziata A. (2009). Effects of Particulate Matter (PM10, PM 2.5 and PM1) on the Cardiovascular System, *Toxicology*, 261, 1-8.

Rasool, K., Pandey, R., Abdul Rasheed, P., Berdiyorov, G., Mahmoud, K. (2019). MXenes for Environmental and Water Treatment Applications. 10.1007/978-3-030-19026-2_22.

Rodriguez-Abreu, C., Vilanova, N., Solans, C., Ujihara, M., Imae, T., López-Quintela, A., & Motojima, S. (2011). A combination of hard and soft templating for the fabrication of silica hollow microcoils with nanostructured walls. *Nanoscale research letters*, *6*(1), 330. https://doi.org/10.1186/1556-276X-6-330

Samet, J. M., Dominici, F., Curriero, F. C., Coursac, I., & Zeger, S. L. (2000). Fine particulate air pollution and mortality in 20 U.S. cities, 1987-1994. *The New England journal of medicine*, *343*(24), 1742–1749. https://doi.org/10.1056/NEJM200012143432401

Saxena, P., Sonwani, S. (2019). Primary Criteria Air Pollutants: Environmental Health Effects. DOI: 10.1007/978-981-13-9992-3_3.

Scherbakova K. (2010). İstanbul'daki solunabilir partikül maddenin boyut dağılımının istatistiksel analizi, Yüksek Lisans Tezi, İstanbul Üniversitesi, Fen Bilimleri Enstitüsü, İstanbul, 282644.

Shi, Y., He, L., Deng, Q., Liu, Q., Li, L., Wang, W., Xin, Z., & Liu, R. (2019). Synthesis and Applications of Silver Nanowires for Transparent Conductive Films. *Micromachines*, *10*(5), 330. https://doi.org/10.3390/mi10050330

Sohn, H., Park, C., Oh, J. M., Kang, S. W., & Kim, M. J. (2019). Silver Nanowire Networks: Mechano-Electric Properties and Applications. Materials (Basel, Switzerland), 12(16), 2526. https://doi.org/10.3390/ma12162526

Sun, Y., Yin, Y., Mayers, B.T., Herricks, T., Xia, Y.(2002). Uniform silver nanowires synthesis by reducing $AgNO_3$ with ethylene glycol in the presence of seeds and poly(vinyl pyrrolidone). *Chem. Mater*. 14, 4736–4745

Taner, S. (2012). İç Ortam Havasındaki Partikül Maddelerin Boyut Dağılımının ve Elementel Kompozisyonunun İncelenmesi, Yüksek Lisans Tezi, Kocaeli Üniversitesi.

Taner, S., Pekey, B., Arslanbaş, D., Pekey, H. (2011). Restoranlarda farklı boyut aralıklarındaki partikül madde konsantrasyonlarının belirlenmesi, *9. Ulusal Çevre Mühendisliği Kongresi*, Samsun, Türkiye.

Tang, X., Yan, X. (2017) Dip-coating for fibrous materials: mechanism, methods and applications. *J Sol-Gel Sci Technol* 81**,** 378–404. https://doi.org/10.1007/s10971-016-4197-7

Tcharkhtchi, A., Abbasnezhad, N., Zarbini Seydani, M., Zirak, N., Farzaneh, S., & Shirinbayan, M. (2020). An overview of filtration efficiency through the masks: Mechanisms of the aerosols penetration. Bioactive materials, 6(1), 106–122. https://doi.org/10.1016/j.bioactmat.2020.08.002

Ulutepe, L. (2007). Hijyenik Ortamların Hava Filtrasyonu, VIII. Ulusal Tesisat Mühendisliği Kongresi, Seminer Bildirisi.

USEPA. (2007a). Terms of Environment:Glossary, Abbreviations and Acronyms.

USEPA. (2007b). "Particulate Matter (PM) Basics | Particulate Matter (PM) Pollution". https://www.epa.gov/pm-pollution/particulate-matter-pm-basics.

Uzunpınar, S. (2022). Doğu Akdeniz Atmosferinde Meteoroloji ve Taşınımın Parçacı Konsantrasyonu ve Boyut Dağılımı Üzerine Etkisi. Yüksek Lisans Tezi, Orta Doğu Teknik Üniversitesi.

Verger, L., Xu, C., Natu, V., Cheng, H., Ren, W., & Barsoum, M.W. (2019). Overview of the synthesis of MXenes and other ultrathin 2D transition metal carbides and nitrides. *Current Opinion in Solid State and Materials Science*. DOI:10.1016/J.COSSMS.2019.02.001

Vijayan, V. K., Paramesh, H., Salvi, S. S., & Dalal, A. A. (2015). Enhancing indoor air quality -The air filter advantage. *Lung India: official organ of Indian Chest Society*, *32*(5), 473–479. https://doi.org/10.4103/0970-2113.164174

Wallace, L. A., Pellizzari, E. D., Hartwell, T. D., Whitmore, R., Sparacino, C., Zelon, H. (1986). Total exposure assessment methodology (team) study: Personal exposures, indoor-outdoor relationships, and breath levels of volatile organic compounds in New Jersey, *Environment International*, Volume 12, Issues 1–4, Pages 369-387, ISSN 0160-4120, https://doi.org/10.1016/0160-4120(86)90051-6

Wang, C., Wu, S., Jian, M., Xie, J., Xu, L., Yang, X., Zheng, Q., Zhang, Y. (2016). Silk nanofibers as high efficient and lightweight air filter. *Nano Res*. 9, 2590–2597. https://doi.org/10.1007/s12274-016-1145-3

Wang, C.X., & Otani, Y. (2013). Removal of Nanoparticles from Gas Streams by Fibrous Filters: A Review. Industrial & Engineering Chemistry Research, 52, 5-17.

WHO. (2016). Air pollution. Retrieved May, 2022 from https://www.who.int/airpollution/en/.

WHO. (2021). Ambient (outdoor) air quality and health. In *WHO*. Retrieved from World Health Organization website: https://www.who.int/en/news-room/fact-sheets/detail/ambient-(outdoor)-air-quality-and-health

Xiao, J., Liang, J. C., Zhang, C., Tao, Y., Ling, G.-W., Yang, Q.-H., Advanced Materials for Capturing Particulate Matter: Progress and Perspectives. *Small Methods* 2018, 2, 1800012. https://doi.org/10.1002/smtd.201800012

Xue, T., Guan, T., Zheng, Y., Geng, G., Zhang, Q., Yao, Y., & Zhu, T. (2020). Long-term $PM_{2.5}$ exposure and depressive symptoms in China: A quasi-experimental study. *The Lancet regional health. Western Pacific*, *6*, 100079. https://doi.org/10.1016/j.lanwpc.2020.100079

Yadav, I. C., Devi, N. L. (2019). Biomass Burning, Regional Air Quality, and Climate Change, *Encyclopedia of Environmental Health (Second Edition)*, Pages 386-391, ISBN 9780444639523, https://doi.org/10.1016/B978-0-12-409548-9.11022-X.

Zhang, L., Song, T., Shi, L. et al. (2021). Recent progress for silver nanowires conducting film for flexible electronics. *J Nanostruct Chem* 11, 323–341. https://doi.org/10.1007/s40097-021-00436-3

Zhang, P., Wyman, I., Hu, J., Lin, S., Zhong, Z., Tu, Y., … Wei, Y. (2017). Silver nanowires: Synthesis technologies, growth mechanism and multifunctional applications. *Materials Science and Engineering B: Solid-State Materials for Advanced Technology*, *223*, 1–23. https://doi.org/10.1016/j.mseb.2017.05.002

Zhang, R.Y.; Hsieh, G.W. (2020). Electrostatic polyester air filter composed of conductive nanowires and photocatalytic nanoparticles for particulate matter removal and formaldehyde decomposition. *Environ. Sci. Nano , 7,* 3746–3758. https://doi.org/10.1039/D0EN00683A

Zhao, X., Holta, D., Tan, Z., Oh, J-H., Echols, I., Anas, M., Cao, H., Lutkenhaus, J., Radovic, M., Green, M. (2020). Annealed Ti3C2Tz MXene Films for Oxidation-Resistant Functional Coatings. *ACS Applied Nano Materials*. 3. 10.1021/acsanm.0c02473.

Zhao, X., Li, Y., Hua, T., Jiang, P., Yin, X., Yu, J., & Ding, B. (2017). Low-Resistance Dual-Purpose Air Filter Releasing Negative Ions and Effectively Capturing $PM_{2.5}$. *ACS applied materials & interfaces*, *9*(13), 12054–12063. https://doi.org/10.1021/acsami.7b00351

Zhu, G., Kremenakova, D., Wang, Y. & Militky, J. (2015).Air permeability of polyester nonwoven fabrics. Autex Research Journal,15(1) 8-12. https://doi.org/10.2478/aut-2014-0019

APPENDICES

A. Outstanding studies regarding the use of nanomaterials in air filtration

Table A1. The literature data on the outstanding studies regarding the use of nanomaterials in air filtration.

Nanomaterial	Result	Reference
Ag NP decorated-silk nanofiber	RE: For $PM_{2.5}$: 98.8% For 300-nm particles: 96.2%	Wang et al. (2016)
Ag NP decorated-silica particles	RE: For bacteria: > 99.99 %	Ko et al. (2014)
Ag NP decorated- PAN nanofiber	RE: For bacteria: 99 %	Selvam and Nallathambi, (2015)
PAN nanofiber	RE: For $PM_{2.5}$: >95 % Pressure drop: 133 Pa	Liu et al. (2015)
Polyimide nanofiber	RE: For $PM_{2.5}$: >99.5 % Pressure drop: 73 Pa	Zhang et al. (2016)
PAN nanofiber	RE: For $PM_{2.5}$: >99 %	Khalid et al. (2017)
Nanopoliethylene with a layer of Ag	RE: For $PM_{2.5}$: 99.6 % Pressure drop: 349 Pa	Yang et al. (2017)
Polyimide-nanofiber	RE: For $PM_{2.5}$: >99.5 %	Liu et al. (2017)

PAN nanofiber	RE: For $PM_{2.5}$: >98.23% For bacteria: >95.2%	Liu et al. (2019)
Carbon nanowire	RE: For $PM_{2.5}$: >95 %	Yang et al. (2019)
Copper nanowire	RE:	Han et al. (2021b)

B. Technical datasheet of H13 class HEPA filter

AFT FILTER

TECHNICAL SPEC. DATASHEET

HEPA FILTER						
Dimensions (mm)			Filter Class (EN 1822)	Filtration Area (m^2)	Nominal Air Flow (m^3/h)	Initial Resistance (Pa)
W	H	D				
140	140	30	H13	0,22	15	100(±10%)

Filtration Media: Micro Glassfiber

Seperator: Thermoplastic Hotmelt

Sealant Type: 2K Poly

Frame Type: Galvanized

Final Pressure Drop: 600 Pa (recommended)

Max. Temperature: 70°C

Max. Humidity: %90 rH

Susuz Mah. Kümeevleri Cad.
No:253/A Yenimahalle / ANKARA
www.aftfiltre.com.tr
info@aftfiltre.com.tr
Tel: 0 312 815 44 34
Faks: 0 312 815 44 77

C. PM_1 removal efficiencies of filters

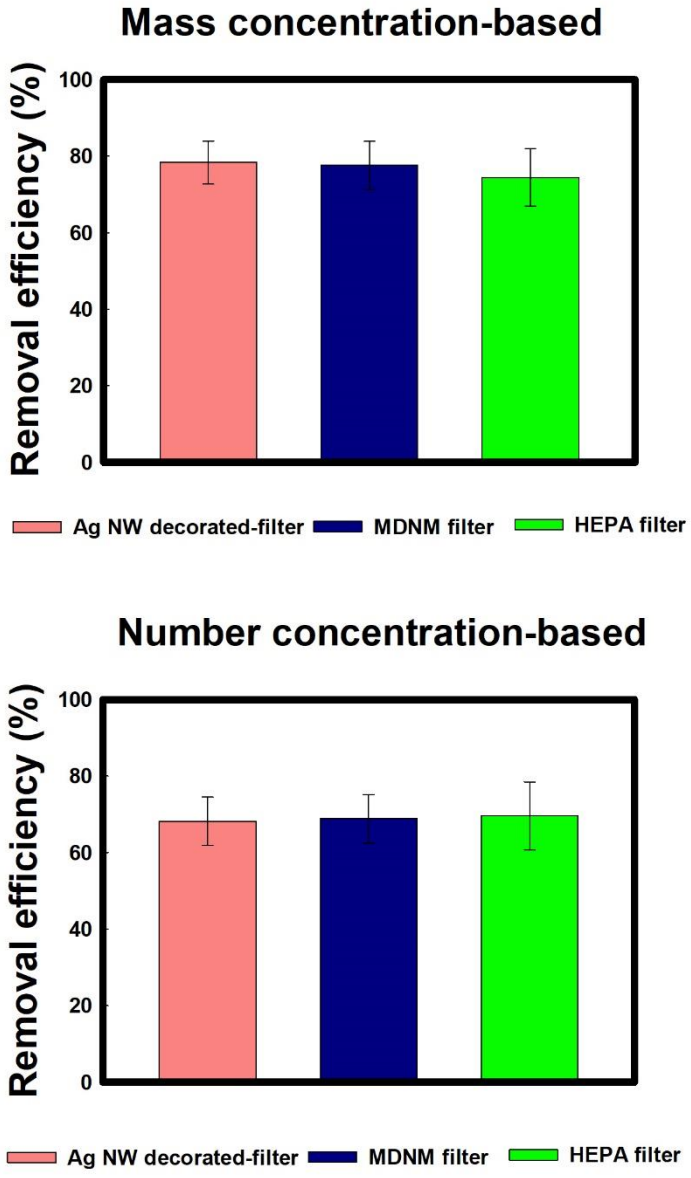

Figure C1. Mass concentration-based and number concentration-based removal efficiencies of nanomaterial-decorated filters and HEPA filter for PM_1.

D. An example of Grimm EDM107 raw data

```
P   21    9   19   12    5   14  100    0  130   62  151  181    0  108  132   0
C_:    6380     1820      680      260      115       80       65       40
C_;      20       15       10       10       10       10       10       10
c_:      10        6        6        6        6        6        5        5  160
c_;       5        3        2        2        2        0        0        0    0
P   21    9   19   12    6   14  100    0  130   49  137  181    0  107  133   0
C_:    7560     2190      795      330      180       95       60       35
C_;      15       15       15       15       10       10        5        5
c_:       5        5        2        0        0        0        0        0  160
c_;       0        0        0        0        0        0        0        0    0
P   21    9   19   12    7   14  100    0  130   48  154  181    0  107  133   0
C_:    7635     2205      770      300      150      110       55       30
C_;      20       20       20       10       10       10        0        0
c_:       0        0        0        0        0        0        0        0  160
c_;       0        0        0        0        0        0        0        0    0
P   21    9   19   12    8   14  100    0  130   47  135  181    0  107  133   0
C_:    6945     1930      590      160       90       40       35       35
C_;      25       20       20       10       10       10       10        4
c_:       4        2        2        1        1        1        1        1  160
c_;       1        0        0        0        0        0        0        0    0
P   21    9   19   12    9   14  100    0  130   47  135  181    0  107  133   0
C_:    7990     2400      795      310      185       95       75       35
C_;      35       25       10        0        0        0        0        0
c_:       0        0        0        0        0        0        0        0  160
c_;       0        0        0        0        0        0        0        0    0
P   21    9   19   12   10   14  100    0  130   46  148  181    0  107  134   0
C_:    7415     1985      650      215      105       35       10        5
C_;       0        0        0        0        0        0        0        0
c_:       0        0        0        0        0        0        0        0  160
c_;       0        0        0        0        0        0        0        0    0
P   21    9   19   12   11   14  100    0  130   46  196  181    0  107  134   0
C_:    7165     2140      710      265      110       45       30       10
C_;       5        5        0        0        0        0        0        0
c_:       0        0        0        0        0        0        0        0  160
c_;       0        0        0        0        0        0        0        0    0
P   21    9   19   12   12   14  100    0  130   46  212  181    0  107  134   0
```